Tampere University

Vilma Lahti

PHOTO-RESPONSE OF PHOSPHATE GLASSES DURING RADIATION TREATMENT

Master of Science Thesis
Faculty of Engineering and Natural Sciences
Examiners: Prof. Laeticia Petit
Dr. Maxime Cavillon
December 2023

ABSTRACT

Vilma Lahti: Photo-response of phosphate glasses during radiation treatment
Master of Science Thesis
Tampere University
Advanced Engineering Physics
November 2023

The goal of this project was to study the effects of laser irradiation on the structural and spectroscopic properties of Er^{3+} doped phosphate glasses with and without silver.

Glasses with the composition (100 – 0.25 – x) (75 $NaPO_3$ – 25 CaF_2) – 0.25 Er_2O_3 – x Ag_2O (in mol-%), where x = 0 or x = 4 were prepared using melting process. After the glasses were annealed, they were polished, and heat treated with the goal to precipitate Er^{3+} doped CaF_2 crystals as well as silver nanoparticles in the glasses. The as-prepared and heat-treated glasses were irradiated after determining the ablation threshold of the glasses and finding out what parameters would be most suited for the irradiation. The surface profiles of the irradiated samples were measured using a profilometer to evidence ablation or expansion/contraction of the glass surface during the radiation treatment. The structural and spectroscopic properties of the irradiated glasses were measured prior and after irradiation.

The glasses irradiated with CO2 laser showed that the crystallization and addition of Ag2O decrease the photosensitivity of the glasses. The formation of the silver nanoparticles causes the glass to become more photosensitive. Signs of contraction of the network is expected to occur when using a fs laser at low pulse energies. The contraction is thought to be due to defect formation as suspected from the changes in the structural and spectroscopic properties of the glasses after irradiation. The glasses do not crystallize nor amorphize as a result of the irradiation. However, silver nanoparticles are suspected to form when using high-power laser irradiation, but only when the glass is heat treated before irradiation.

In this project, we were able to show that the growth of silver nanoparticles is possible with a CO_2 laser, but the preparation of the samples needs to be optimized to achieve more consistent results.

Keywords: glass, CO_2 laser, fs laser, glass-ceramic, phosphate glass

TIIVISTELMÄ

Vilma Lahti: Fosfaattilasien valonherkkyysominaisuudet säteilytys käsittelyn aikana
Diplomityö
Tampereen yliopisto
Teknillinen fysiikka
Marraskuu 2023

Projektin tavoitteena oli tutkia lasersäteilytyksen vaikutuksia hopealla ja ilman valmistettujen Er^{3+} ioneilla seostettujen fosfaattilasien rakenteellisiin ja spektroskooppisiin ominaisuuksiin.

Lasit, jotka olivat koostumukseltaan (100 – 0,25 – x) (75 $NaPO_3$ – 25 CaF_2) – 0.25 Er_2O_3 – x Ag_2O (mooli-%), jossa x = 0 tai x = 4 valmistettiin sulatus menetelmällä. Kun lasit oli hehkutettu, ne hiottiin ja lämpökäsiteltiin tavoitteena saostaa Er^{3+} seostettuja CaF_2-kiteitä ja hopeananopartikkeleita laseissa. Käsittelemättömät ja lämpökäsitellyt lasit säteilytettiin sen jälkeen, kun lasien ablaatiokynnys oli määritetty ja saatu selville, mitkä parametrit sopisivat parhaiten säteilytykseen. Säteilytettyjen näytteiden pintaprofiilit mitattiin profilometrillä, jolla todistettiin lasipinnan ablaatio tai laajeneminen/ supistuminen säteilytyksen aikana. Säteilytettyjen lasien rakenteelliset ja spektroskooppiset ominaisuudet mitattiin ennen käsittely sekä käsittelyn jälkeen.

CO_2-laserilla säteilytetyt lasit osoittivat, että kiteytyminen ja Ag_2O:n lisääminen vähentävät lasien valoherkkyyttä. Hopeananopartikkeleiden muodostuminen saa lasin muuttumaan valoherkemmäksi. Merkkejä supistumisesta odotetaan esiintyvän, kun käytetään fs-laseria matalilla pulssienergioilla. Supistumisen arvellaan johtuvan defektimuodostumisesta lasien säteilytyksen jälkeisien rakenteellisten ja spektroskooppisten ominaisuuksien muutoksien perusteella. Lasit eivät kiteydy eivätkä amorfisoidu säteilytyksen seurauksena. Hopeananopartikkeleita kuitenkin epäillään muodostuvan käytettäessä suuritehoista lasersäteilytystä, mutta vain silloin, kun lasi on lämpökäsitelty ennen säteilytystä.

Tässä projektissa pystyimme osoittamaan, että hopeananopartikkeleiden kasvu on mahdollista CO_2-laserilla, mutta näytteiden valmistelu on optimoitava johdonmukaisempien tulosten saavuttamiseksi.

Avainsanat: lasi, CO_2 laser, fs laser, lasikeraami, fosfaatti lasi

PREFACE

This thesis was made as a part of a Master Programme in Science and Engineering at Tampere University. The experiments were conducted under the supervision of Laeticia Petit in the Photonic Glasses research group in the Laboratory of Photonics. The research was done during the second half of 2022 and writing was done during 2023.

I want to thank Professor Laeticia Petit for guidance, support and understanding during this project. I would also like to thank Dr. Maxime Cavillon for the irradiation with the fs laser of the samples and analysis as well as FabLab facilities for allowing me to use their CO_2 laser for this project. Thank you to Mikko Hongisto for the help and tips in use of the CO_2 laser and Turkka Salminen for the help with the confocal Raman microscope. A huge thank you to my fiancé, Pinja, for believing, supporting and motivating me during the writing process of this thesis. And lastly thank you to my cat Esko for the not so helpful contributions to writing my thesis (unfortunately I had to delete everything he wrote).

Tampere, 21 November 2023

Vilma Lahti

CONTENTS

LIST OF FIGURES

LIST OF SYMBOLS AND ABBREVIATIONS

3D	Three-dimensional space
BCE	Before the Common Era
dpi	Dots per inch – unit of resolution
ET	Energy transfer
GC	Glass-ceramic
MNP	Metallic nanoparticles
mol-%	Mole percent
NI	Nonirradiated
NP	Nanoparticles
PL	Photoluminescence
POHC	Phosphorus–oxygen hole center
RE	Rare-earth
UV	Ultraviolet

ΔJ	Change in rotational angular momentum
Δn	Change in refractive index
Q^n	Q-notation, n denotes number of linked oxygen
T_g	Glass transition temperature
T_p	Crystallization temperature
v_0	Frequency of the incident beam
v_m	Vibrational frequency of a molecule

.

1 INTRODUCTION

Lasers are a big part of today's world. Everybody is probably familiar with some form of lasers, such as laser pointers but they are actually very widely used in all kinds of application in technology, medicine, research, etc. Some examples of these applications are optical spectroscopy, welding, and data transmitting. (Yamane & Asahara, 2000) (Schauer, 2021) Lasers can be used to modify materials for example by cutting, scribing, or abrasion. (Yamane & Asahara, 2000) Also, the properties of materials such as glasses can be modified.

Glasses doped with rare-earth (RE) ions are especially interesting and used in many scientific applications. RE doped glasses are excellent amplifiers and thus they have great potential in optical applications. (Yamane & Asahara, 2000) The spectroscopic properties of RE doped glasses can be enhanced by making them into glass-ceramics (GC). (Gonçalves, Santos, & Almeida, 2002) Metallic nanoparticles can be used along RE elements to enhance the spectroscopic properties even more; they absorb light very efficiently and can transfer energy to RE ions. (Kassab, da Silva, & de Araújo, 2010) (Mahraz, Sahar, Ghoshal, Dousti, & Amjad, 2013)

Glass-ceramics can be formed, and nanoparticles grown using thermal treatments (Höland & Beall, 2019) (Mody, Siwale, Singh, & Mody, 2010). This thermal treatment however affects the whole glass sample. Lasers could be used to locally induce these changes. This way, the crystallization and nanoparticles could be obtained locally, in areas where they are needed or wanted in a controlled manner.

In this thesis, glasses with the composition of $(100 - 0.25 - x)\ (75\ NaPO_3 – 25\ CaF_2) - 0.25\ Er_2O_3 – x\ Ag_2O$, where x = 0 or x = 4 in mol-% are prepared using standard melting process. The glasses are then irradiated, and the induced changes are analysed.

Chapter 2 of this thesis is about the background of glasses and glass-light interaction. This chapter explains what glasses and laser glasses are. Lasers used to irradiate the glasses are also explained as well as the changes the irradiation can cause.

Chapter 3 explains how the glasses studied in this thesis were prepared. The irradiation of the glasses is explained along with the laser setups used for the irradiation. The methods and equipment used to analyse the glasses are introduced.

The results of the analysis of the glasses are presented and discussed in chapter 4. The as-prepared glasses are characterized before and after irradiation. The photo-response of the glasses irradiated with both CO_2 and fs lasers are discussed.

And finally, chapter 5 concludes the thesis and provides future plans for the continuation of this project.

2 THEORETICAL BACKGROUND

2.1 Glass

Glasses are hard but brittle amorphous solids that do not have long range, periodic structure. Glasses have a temperature region where they exhibit glass transformation behaviour. It is believed that the first glasses were formed accidently from sand (SiO_2) and silica-based glasses have stayed the most common and the most used glasses throughout history. Humans started to produce glass as early as 7000 BCE in Egypt and used glass in tools and weapons even earlier by shaping naturally occurring obsidian. Today glasses can be formed from plethora of different compositions and with multiple different methods and can be used for multiple applications such as windowpanes, kitchen glassware, electronics, optical fibres, and many others. (Shelby, 2005)

2.1.1 Glass formation

The traditional way to form a glass is to cool it from a melt, but even methods that do not require melting exist, such as sol-gel and vapor deposition processes for example. (Shelby, 2005)

As mentioned before, all substances that exhibit a glass transformation behaviour are glasses. This behaviour can be seen at the temperature region called glass transformation range, which can be seen in Figure 1 where the enthalpy of a material is shown as a function of temperature.

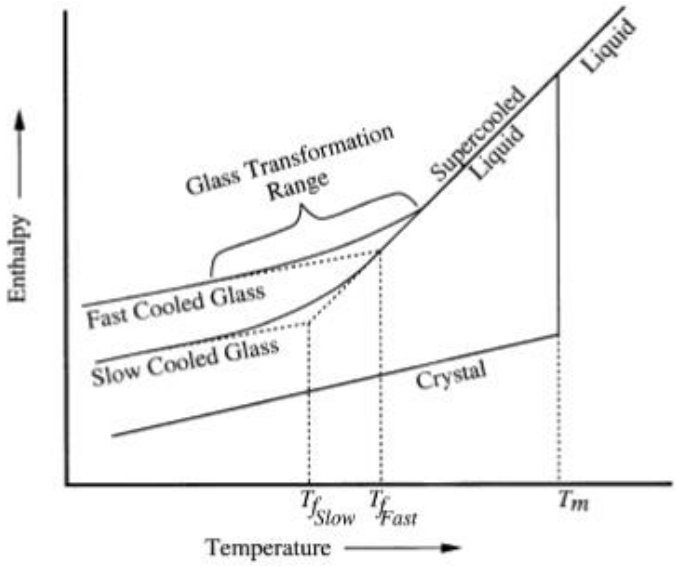

Figure 1. A diagram depicting the formation of glass. (Shelby, 2005)

When a material is cooled down, its atomic structure changes and if it does not crystallize when cooled below its melting temperature, the material turns into a supercooled liquid. The enthalpy continues to gradually decrease when the liquid is cooled further, and the viscosity of the liquid starts to increase. When the viscosity of the liquid becomes high, the complete rearrangement of the atoms is no longer possible, and the structure is not able to reach the equilibrium liquid structure. This also causes the enthalpy to gradually curve from the equilibrium line as well. Eventually the viscosity becomes so great, the structure becomes fixed, and the enthalpy starts to follow the heat capacity of a frozen solid. Between the enthalpy of the equilibrium liquid and the frozen solid is the region of the glass transformation. (Shelby, 2005)

The properties of the glass can be modified by changing the composition of the glass to fit the application they are made for. (Shelby, 2005) The component used in glass batches can be divided into different categories:

- **Formers** are the most important components, and they make up the main structure of the glass. Formers are cations that bond with oxygen and they are able to produce good glasses. Some of the most common formers are Si from silica (SiO_2), B from boric oxide (B_2O_3), and P from phosphoric oxide (P_2O_5) and these are able to produce glasses all by themselves. Some compounds can also act as formers but cannot readily produce good glasses by themselves but when mixed with other oxides. Examples of these are Bi_2O_3 and TeO_2. There can be multiple different formers in a batch, for example chalcogenide glasses are formed from S, Se and Te. (Shelby, 2005)
- **Modifiers** are cations with very low electronegativities that form highly ionic bonds with oxygen. They can never form glasses on their own but can be used to modify the properties of the glass batch they are added to by modifying the structure of the network. Modifiers can be used to lower the production cost of a glass, increase the chemical durability or for example lower the melting temperature of a glass such as silica which has a melting temperature of over 2000°C. When a modifier is added into silica batch, the melting temperature can be lowered to a much more reasonable 1600°C. Modifiers are compounds such as Na_2O, and Li_2O among others. (Shelby, 2005)
- **Intermediates** are cations that behave intermediate between formers and modifiers, hence the name. They have slightly lower electronegativities than formers and thus form slightly more ionic bonds with oxygen. Intermediates can partially

replace former cations in the glass network but cannot form glasses by on their own. Al can also be considered as an intermediate. (Shelby, 2005)

- **Colorants or dopants** are mostly 3d transition metals or rare-earths and they are used to affect the colour of the glass. Before they were discovered to be radioactive, uranium oxides were widely used as colorants. Silver and gold form colloids in glasses which act as colorants. (Shelby, 2005)
- **Fining agents** are used to remove bubbles from the glass melt. They include compounds such as NaCl, CaF_2 and NaF. (Shelby, 2005)

As mentioned before, silica-based glasses are the most common glasses. It has a network that is composed of SiO_4 units with tetrahedra structure where a Si^{4+} ion is surrounded by four O^{2-} ions. In the glass network, the units share all four of its O^{2-} ions with their neighbouring groups. (Ohring, 1995) Silica glasses have been used as optical materials because of their good optical properties such as low thermal expansion, large transparency range and high refractive index homogeneity. Some applications for them are optical fibres and deep UV lens elements. Silica glasses can be easily manufactured in large sizes, which also is a big reason they are so popular and widely used. (Moore & Smith, 2022) However, silica glasses have very high melting temperature, and they have a poor rare-earth element solubility, drawbacks which have led to the development of glass compositions.

In this project phosphate glasses were used. This is because phosphate glasses can be melted in relatively low temperatures, they have high optical properties and thermal expansion coefficient, as well as excellent rare-earth solubility (Karabulut, et al., 2001) (Veselský, et al., 2021). Compared to silicate glasses, phosphate glasses also have low dispersion and relatively high refractive indices. Phosphate forms a tetrahedra structure group where the phosphorus is surrounded by the oxygens and the groups are linked together by the bridging oxygens. The groups can have various different number of bridging oxygens: Q^3 tetrahedral site has three bridging oxygens (BO) that connect to the adjacent groups, Q^2 with two BO, Q^1 with one BO, and finally Q^0 with only non-bridging oxygen (NBO). Glasses with a large number of Q^3 units have a cross-linked network whereas glasses with a large number of Q^2 are formed by metaphosphate chains that are polymer-like. Pyro- (Q^1) and orthophosphate (Q^2) anions form ‘invert’ glasses. The ratio of oxygen and phosphorus in the glass composition determines which of these tetrahedral sites are formed. (Brow, 2000)

2.1.2 Er^{3+} doped glass

Laser glasses are obtained by adding rare-earth (RE) ions in the glass matrix. These ions can absorb or emit radiation. (Yamane & Asahara, 2000) When a photon is absorbed, the atom becomes excited and the decay of this excited state results in a photon being emitted (Demas & Demas, 2001). Rare-earth (RE) doped glasses are excellent for lasing, amplification and conversion applications. The composition of the glasses can be tailored so when doped with RE, they can have high absorption and emission cross-sections leading to enhancement of the amplification and conversion of light properties. Er^{3+} doped phosphate glass with the composition (75 $NaPO_3$-25 CaF_2) (in mol%) was used in this study due to its good optical properties and high RE ion solubility (Ohja, Dmitrieva, Blanc, & Petit, 2021).

2.1.2.1 Er^{3+} doped glass-ceramics

Crystals with specific crystalline phase are known to exhibit better spectroscopic properties than glasses (Gonçalves, Santos, & Almeida, 2002). They are however difficult and expensive to prepare, so there has been a lot of interest in preparing glasses that contain RE doped crystals. (Ohja, Dmitrieva, Blanc, & Petit, 2021) (Nommeots-Nomm, et al., 2018)

Crystals can be grown in glass using a thermal treatment. The material is then called glass-ceramic (GC). They were originally discovered accidentally in mid-1950s by Dr. Stookey, when the furnace he used to heat his glasses overheated. GCs have been desired ever since because of their superior thermal, biological, chemical, and dielectric properties compared to metals and organic polymers. (Höland & Beall, 2019) Glass-ceramics can be used in variety of applications, such as electronics, dinnerware, medicine, and optical materials. (Gonçalves, Santos, & Almeida, 2002)

GCs are usually produced using two-step process: nucleation and crystal growth. In order for the crystals to grow to a detectable size, it requires nuclei, defined as the seeds for crystallization. The nuclei are grown by heat treating the glasses above their glass transition temperature (T_g). The nucleation can be favoured by adding nucleating agents in the glass, such as silver or copper, for example. Nuclei cannot grow if the temperature is increased within the Metastable zone of undercooling which is presented in Figure 2. (Shelby, 2005)

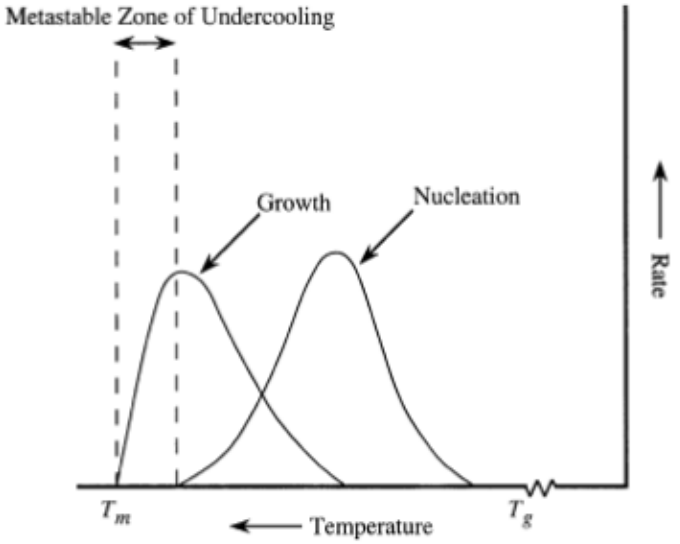

Figure 2. Illustration of the rates of nucleus and crystal growth as a function of temperature. (Shelby, 2005)

However, the crystal growth occurs when using a temperature near the crystallization temperature (T_p). In this process the crystalline phase starts to form around the nuclei. (Shelby, 2005)

The temperatures used for the nucleation and growth depend on the glass composition and need to be determined experimentally by measuring the thermal properties of the glasses.

Er^{3+} doped GCs have been studied extensively and they have been seen to improve the luminescence properties of the Er^{3+} ion while maintaining good glass stability and easy fabrication process. (Gonçalves, Santos, & Almeida, 2002) In the $75NaPO_3$-$25CaF_2$ glass system, the Er^{3+} ions incorporate with the CaF_2 crystals which precipitate in the volume of the glass during a thermal treatment leading to an in-crease in the upconversion properties (Szczodra, Mardoukhi, Hokka, Boetti, & Petit, 2019).

2.1.2.2 Metallic nanoparticles in Er^{3+} doped glass

Metallic nanoparticles (MNP) are nanoscale particles or clusters formed from metal (Blackman, 2009). They can be grown in the glass during a thermal treatment. MNPs have been a huge interest among scientists due to their many applications in nanotechnology and they are especially used in biomedical sciences and engineering. For example, MNPs are used in the medical field in targeted drug delivery, diagnostic imaging, and even cancer therapy. (Mody, Siwale, Singh, & Mody, 2010) In engineering they can be used in lasers, optical amplifiers, etc. (Kassab, da Silva, & de Araújo, 2010).

In rare-earth (RE) doped glasses, MNPs can be used to enhance the photoluminescence (PL) of the RE ions. The MNPs confine the local electromagnetic field in the vicinity of themselves, and thus also the RE ions close to them, enhancing the field. They also absorb light efficiently and transfer the absorbed energy to the RE ions as illustrated in Figure 3. (Kassab, da Silva, & de Araújo, 2010) (Mahraz, Sahar, Ghoshal, Dousti, & Amjad, 2013)

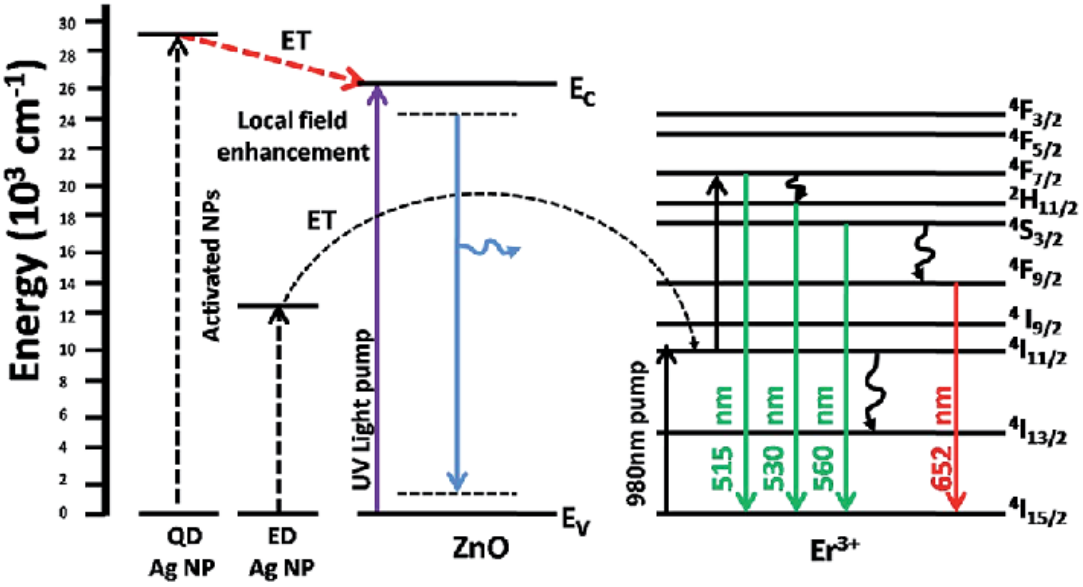

Figure 3. Illustration of energy transfer from Ag NP to Er^{3+} ion. From (Das, Phadke, Khichar, & Chawla, 2014)

Qi, et al reported that the fluorescence from Er^{3+} was 7 times higher in bismuth glasses when prepared with Ag NPs. This is believed to be a result of local field enhancement from surface plasmon resonance. (Qi, et al., 2013) There has also been reports of increase in the upconversion in Er^{3+} doped tellurite glasses that contain Ag NPs (Mahraz, Sahar, Ghoshal, Dousti, & Amjad, 2013). However, Mahraz, et al. also reported seeing luminescence quenching which is a result of energy transfer from the Er^{3+} to the nanoparticles as seen in Figure 4.

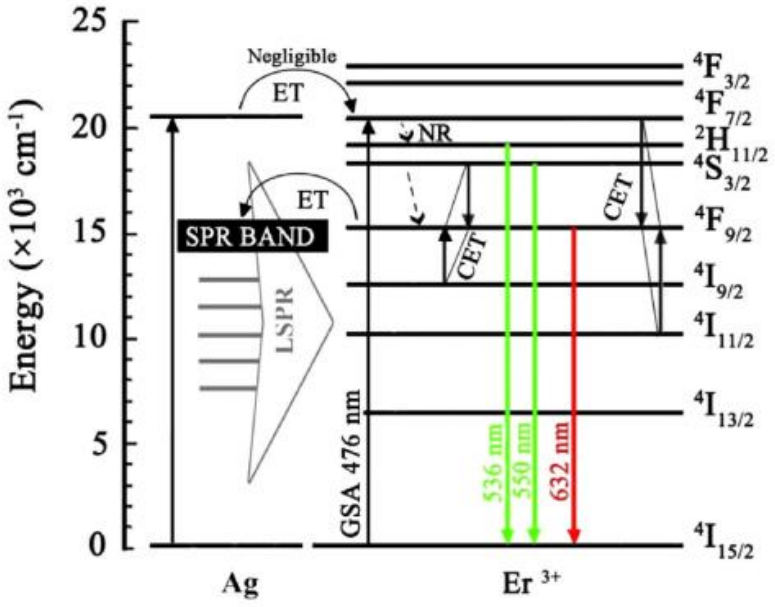

Figure 4. Energy level diagram illustrating energy transfer (ET) from Er^{3+} to Ag NPs. From (Mahraz, Sahar, Ghoshal, Dousti, & Amjad, 2013).

Shestopalova, et al. studied how the addition of Ag_2O in the Er^{3+} doped $75NaPO_3$-$25CaF_2$ glass impacts its thermal properties. The Er^{3+} sites remained unchanged even though the phosphate network was depolymerized by the addition of Ag_2O. There was an increase in the thermal properties of the glass system and the volume precipitation of the CaF_2 crystals was not impacted by the addition of Ag_2O, but it is suspected to limit their precipitation. Smaller crystals are expected in the Ag containing glass. During heat treatment, Ag nanoparticles were found to precipitate on the surface of the glasses. (Shestopalova, et al., 2023)

2.2 Glass-light interaction

There is a large variety of lasers with large range of powers (from milliwatts to hundreds of kilowatts). This is why they can be used in a variety of applications such as in scientific research, manufacturing, and medicine. (Laser Focus World, 2016) In material processing, the CO_2 lasers are commonly used to cut and engrave materials because of their well-focused beam. This has also been utilised in research for example to fabricate microlenses on the surface of glass (Andreeta, Cunha, Vales, Caraschi, & Jasinevicius, 2011). Femtosecond lasers can be used to alter materials physical and chemical properties which makes them excellent for laser direct writing. (Niazi & Doroodgar, 2022)

2.2.1 Lasers

2.2.1.1 CO_2 laser

The CO_2 laser was invented by C. Kumar N. Patel in 1964. It is still one of the most useful laser types today because it has high power and the wavelength it operates in. CO_2 lasers most commonly emit at 10.6 or 9.6 µm but overall, they can be found in the range of 9-11 µm. Many non-metallic materials absorb well in this range which makes CO_2 lasers optimal for atmospheric transmission, material processing and spectral analysis. There has also been development in pulsed CO_2 lasers that are capable of high peak powers and fast pulses without expensive external modulation techniques. (Laser Focus World, 2016)

A schematic of a CO_2 laser is presented in Figure 5.

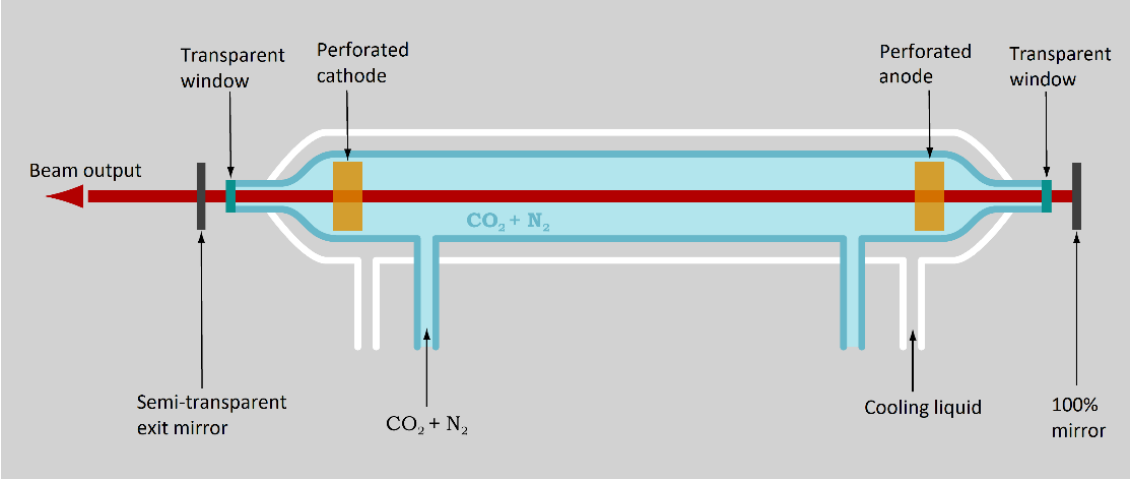

Figure 5. Schematic of a CO_2 laser. Modified from (Brierre, 2009).

The active medium in the CO_2 laser is typically a gas mixture with CO_2 that is electrically discharged. This gas mixture usually consists mainly of CO_2, helium, and nitrogen. The laser transition happens in exited CO_2 molecules. The CO_2 molecules are excited by energy transfer from nitrogen molecules that have been excited to a metastable vibrational level by the electric discharge. This method is much more efficient than exciting the CO_2 directly. The helium helps the removal of heat and the depopulation of the lower laser levels. Excess heat is also mitigated by cooling the gas tube with a cooling liquid. (Patel, 1964) (RP Photonics Encyclopedia, 2005)

The CO_2 laser has such a wide range of possible wavelengths because of its vibrational states. CO_2 molecules have two different vibrational states that can serve as the lower energy state. For every vibrational state, there exist numerous rotational states which

result in many sub-levels. In addition, dipole transitions add two more possible final vibration levels; $\Delta J = 1$ also known as R branch gives higher photon energies and $\Delta J = -1$ or P branch gives lower energies. A CO_2 laser can be made to lase one of these dozens of transitions, but the discrete rotational states of molecules prevent continuous wavelength tuning. To ensure that there are no jumps from one transition to another or lasing on few transitions at the same time during operation, a wavelength-selective element needs to be used. (RP Photonics Encyclopedia, 2005)

There are multiple types of CO_2 lasers with their unique strengths and weaknesses:

- **Sealed-tube and no-flow lasers** are compact lasers with a very high beam quality. In these lasers, inside a sealed tube are the laser bore, and gas supply. The waste heat is reduced by slow gas flow or by diffusion into the walls of the tube. The gas in the tube needs to be continuously regenerated, but the operation lifetimes of these lasers can be several thousands of hours. These lasers produce a few watts to several hundred watts of power. (RP Photonics Encyclopedia, 2005)
- **Diffusion-cooled slab lasers** are capable of producing several kilowatts of output power with reasonable beam quality. In these lasers, the gas is located between two water-cooled radiofrequency electrodes which take up the excess heat. To increase efficiency, an unstable resonator is used. (RP Photonics Encyclopedia, 2005)
- **Fast axial and fast transverse flow lasers** have high beam quality and are also able to produce multiple kilowatt continuous-wave powers. Transverse flow lasers can reach even higher output power at the expense of beam quality. The discharge gas is used to remove excess heat by passing it through an external cooler at a high flow rate. (RP Photonics Encyclopedia, 2005)
- **Transverse excited atmosphere lasers** have a gas pressure of about one atmosphere. The gas is excited with transverse excitation using many electrodes along the tube to avoid extremely high voltages in longitudinal excitation. The high pressures mean that the gas discharge is not stable and thus these lasers only work as pulsed lasers. Typically, these lasers produce around hundred watts of power but can be made for higher powers as well (10 kW). (RP Photonics Encyclopedia, 2005)
- **Gas dynamic CO_2 lasers** do not get their power from a gas discharge but from a chemical reaction. They are a kind of chemical laser fit for multiple megawatts of output power. (RP Photonics Encyclopedia, 2005)

In this study, the radiation treatment was performed using Epilog Laser Fusion M2 40 laser system. This system uses air-cooled laser tubes.

2.2.1.2 Fs laser

Fs lasers are pulsed lasers with a pulse duration in the femtosecond domain. They are categorised as ultrafast lasers along with picosecond lasers. Light pulses below picosecond are generated with passive mode locking technique. (RP Photonics Encyclopedia, 2005) In short, this technique means that a saturable absorber is used in the laser resonator to selectively amplify high-intensity light and absorb low-intensity light leading to mode locking of the laser after multiple round trips of the light pulse (RP Photonics Encyclopedia, 2006). An example of a femtosecond laser setup is illustrated in Figure 6.

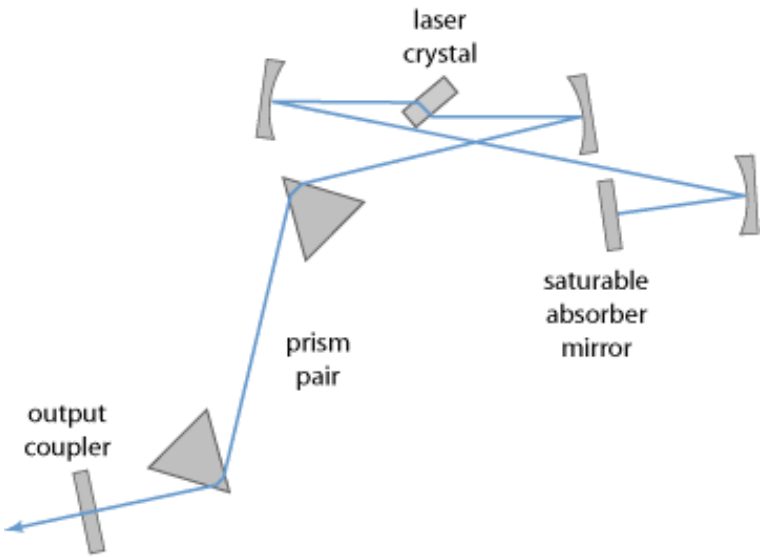

Figure 6. Schematic of an example of femtosecond laser. (RP Photonics, 2023)

Femtosecond lasers are extremely precise due to the laser pulses having short electron-phonon coupling time when interacting with matter. This makes the area affected by the heat small. Long-pulsed and continuous wave lasers work by linear single-photon electron excitation which means that to excite a single electron, energies higher than the band gap of the material are needed.

Femtosecond lasers work by using non-linear electron excitation. This mechanism is unique to ultrafast lasers, and it allows femtosecond lasers to have strong absorption. Non-linear absorption works also on transparent materials such as glass and because of the high-density absorption of photons, the laser can only interact with transparent matter at the focal point. This means even more precision as out-of-focus absorption is not possible as illustrated in Figure 7. (Niazi & Doroodgar, 2022)

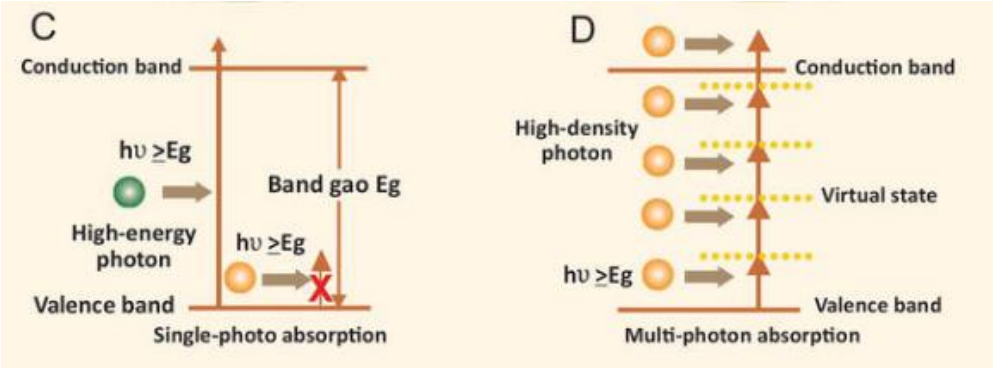

Figure 7. Single-photon (C) and multi-photon (D) absorption mechanisms. From (Niazi & Doroodgar, 2022)

Non-linear absorption can occur from electron avalanche ionization or multiphoton ionization (see Figure 8). The latter usually becomes dominant when pulse duration decreases. (Zoubir, 2004)

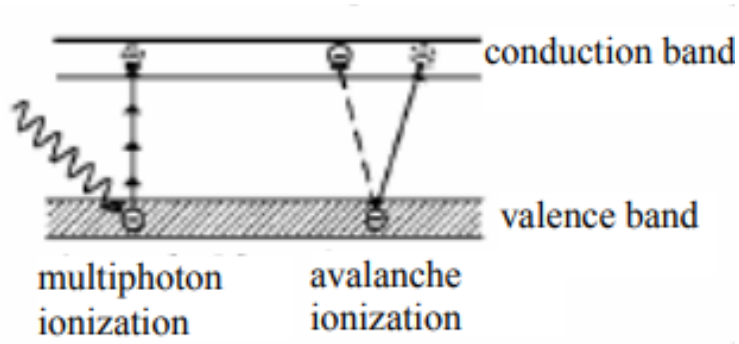

Figure 8. Multi-photon and avalanche ionization mechanisms. (Zoubir, 2004)

Multi-photon ionization means that the material absorbs enough photons simultaneously that the ionization potential is overcome, and an electron is excited to the conduction band. In electron avalanche, ionization conduction-band electrons are oscillating because of the laser field. This causes the electrons to transfer energy. When an electron in the valence band receives enough energy, it will be excited to the conduction band. When the free electrons collide with the lattice, it can cause another valence electron to be excited. This leads to a cumulative growth effect when each excited electron vibrates causing ionization of valence electrons. (Zoubir, 2004)

Due to all their advantages, femtosecond lasers have a resolution beyond the diffraction limit. For multiphoton absorption, a narrower absorbed energy distribution is a result of the Gaussian spatial profile of the beam intensity. (Niazi & Doroodgar, 2022)

Femtosecond laser types are the following:

- **Solid-state Bulk lasers** typically have a pulse duration of 30 fs – 30 ps and pulse repetition rate of 50 – 500 MHz. Diode-pumped lasers can have output powers of 100 mW – 1 W. There are some lasers that are capable of even shorter pulse durations, such as titanium-sapphire lasers which can produce pulses as short as 5 fs and have an output power of 1 W. (RP Photonics Encyclopedia, 2005) This is due to the advanced dispersion compensation that works by cancelling out the chromatic dispersion of some optical elements (RP Photonics, 2007).
- **Fiber lasers** usually have a pulse duration of 50 – 500 fs and repetition rates of 10 – 100 MHz. They usually have between a few milliwatts and tens of milliwatts of output powers. Higher powers can be achieved with stretched-pulse fiber lasers or by using a fiber amplifier, for example. The strong optical nonlinearities of fiber lasers cause the production to require more effort, but fiber lasers can still be quite cost-effective. (RP Photonics Encyclopedia, 2005)
- **Dye lasers** have pulse duration of around 10 fs. They operate in various different wavelengths depending on the dye laser. (RP Photonics Encyclopedia, 2005)
- **Semiconductor lasers** can have pulse durations in the femtosecond domain. Mode-locked semiconductor lasers can produce repetition rates of up to hundreds of gigahertz. Pulse energies are usually around a picojoule. (RP Photonics Encyclopedia, 2005)

In this study, the radiation treatment was performed using Satsuma by Amplitude Systems. It has a pulse duration of 250 fs and repetition rate from single shot to 40 MHZ.

2.2.2 Glass photoresponse

The irradiation causes various changes in the glass due to the light-matter interaction.

2.2.2.1 Structural changes

There are multiple types of changes that can occur.

Some of the changes are not wanted, such as ablation. Ablation means that material is removed from the sample (Harilal, Freeman, Diwakar, & Hassanein, 2014). This occurs when using high power and/or long radiation treatment.

One of the main changes that can occur during radiation treatment is structural changes and more specifically induced refractive index change Δn. It has been reported in multiple studies that Δn is laser dose and material dependant (Zoubir, 2004) (Choi, 2009). If the

refractive index is increased, light can be guided though the irradiated area and be used as a waveguide (Choi, 2009). However, if the refractive index is decreased, the light is guided in the surrounding area. (Zoubir, 2004) The mechanism behind the change in the refractive index is not fully understood in all optical materials, but there have been studies on some materials with suggested glass-light interaction mechanisms (Choi, 2009). Chan, et al. found that after irradiation, the refractive index of silica glass increased due to the formation of various defects in the silica network (Chan J. W., Huser, Risbud, & Krol, 2001). Fernandez, et al. reported that in tellurium glasses the Δn is caused by the migration of elements: tellurium migrates towards the irradiated areas resulting in an increase of the refractive index. At the same time, sodium migrates towards tellurium leading to deficient areas where the refractive index is lowered. (Fernandez, et al., 2014) The refractive index profiles of most phosphate glasses after irradiation are quite complex (Ams, et al., 2008). In phosphate glasses, irradiation has been reported to decrease the refractive index and to lower the density of the irradiated area (Bhardwaj, et al., 2005) (Chan J. W., Huser, Risbud, Hayden, & Krol, 2003). Some phosphate glasses have however been successfully irradiated to obtain positive refractive index changes, for example, Zn-containing phosphate glasses (Fletcher L. , et al., 2011).

Irradiation can form different kinds of defects in glass, such as colour-centre formation. These centres increase absorption and cause colouration in the glass. In addition, electron and hole centres can be formed using laser irradiation. (Zoubir, 2004) Defect formation seems to increase when adding Zn, S or Ag in glass for example (Möncke, Reibstein, Schumacher, & Wondraczek, 2014).

Another common change caused by irradiation is the expansion or contraction of the glass structure. The expansion of the glass which is a result of the density of the glass decreasing causes the refractive index to increase (Zoubir, 2004). Just like the change in refractive index, expansion and contraction is laser dose and material dependant. Choi, et al. reported that the $As_{36}Ge_6S_{58}$ glass exhibits photo-expansion upon irradiation. Their study also showed that new bonds were created with the irradiation, and this would likely be the reason for the expansion. (Choi, 2009) In phosphate glasses the photo-expansion of the glass is suspected from the shift in the Raman band related to the stretching of Q^2 phosphate tetrahedra units. (Fletcher L. , et al., 2009)

Photo-expansion and contraction can be a very useful mechanism. Indeed, Andreeta, et al. used it to form microlenses on the surface of a glass using a CO_2 laser. These lenses were the result of stress relieve and decrease in the density of the glass.

2.2.2.2 Localized formation of crystals/metallic nanoparticles

Crystallization is traditionally obtained by heat treating the glass (Höland & Beall, 2019). Laser irradiation allows for the controlled growth of crystals which are quite desired feature because of their non-linear and electro-optic properties (Muzi, et al., 2021). With laser irradiation, the direction of the crystal growth can be controlled. The high repetition rate of the laser causes ultrafast heating in the glass as well as localized melting. This causes local atom or ion diffusion, non-local material transformation and chemical changes in the glass. (Dubov, et al., 2014) In RE glasses, the rare-earth ion dopants absorb the energy when irradiated and heat up causing crystallization. The RE elements can enter the formed crystal lattice. Crystallization can also form by multiphoton absorption even without dopants. (Hongisto, et al., 2020) It has been possible to form single and 3D ferroelectric crystallization with laser irradiation when parameters were optimized (Stone, et al., 2009).

Radiation treatment can also be used to locally form MNPs. An example of laser-induced silver NP clusters in phosphate glass is shown in Figure 9.

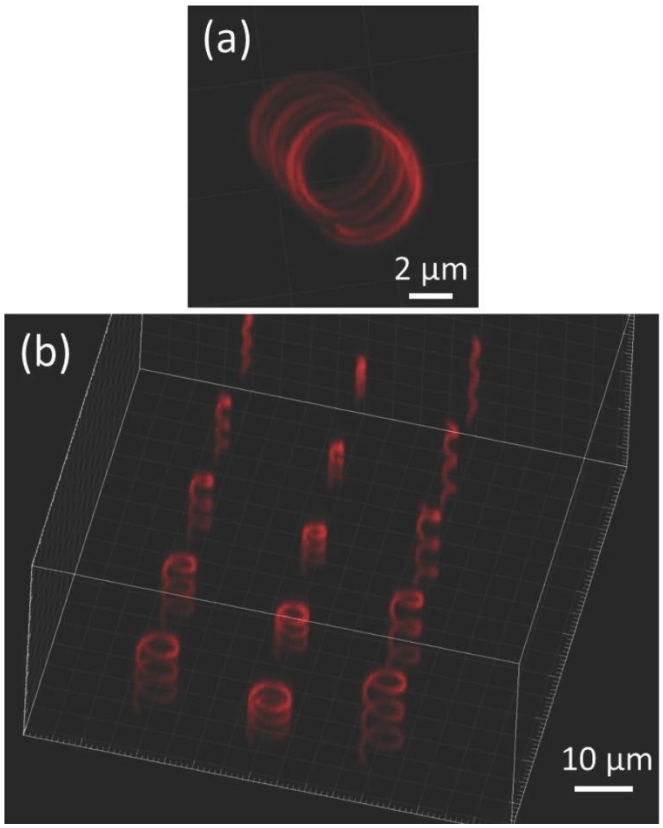

Figure 9. Fluorescence microscope image of 3D-laser induced Ag_0 silver clusters. From (Marquestaut, et al., 2014)

As explained in previous section, traditionally metallic nanoparticles are formed using a heat treatment and in this case the nanoparticles can form anywhere in the sample. Irradiation is an easier way to form and dissolve MNPs locally (Choi, 2009). It is faster and more efficient than thermal treatment. The MNPs will have homogenous size and arrangement, and the laser treatment does not cause additional stress in the glass like the traditional heat treatment method does. (Hofmeister, Thiel, Dubiel, & Schurig, 1997) Laser irradiation is a great way to better control and optimize the optical properties of the particle containing glasses. Irradiation produces free electrons which reduce the metallic ions in the irradiated areas and can lead to aggregation of clusters (Choi, 2009). These clusters can then act as nucleation centres where MNPs can aggregate (Petit, 2019). Annealing or heat treating the glass after irradiation can further help grow the metallic nanoparticles (Choi, 2009).

The goal of this study is to try to locally form/dissolve CaF_2 crystals and Ag NPs in Er^{3+} doped phosphate glass using laser irradiation.

3 MATERIALS AND METHODS

3.1 Preparation

Glasses with the composition $(100 - 0.25 - x)(75\ NaPO_3 - 25\ CaF_2) - 0.25\ Er_2O_3 - x\ Ag_2O$, where $x = 0$ or $x = 4$ in mol-% (labelled Ag0 and Ag4 respectively), were prepared using the melt quenching method. The raw materials used were $(NaPO_3)_6$ (Alfa Aesar, tech.), CaF_2 (Alfa Aesar, 99.95%), Er_2O_3 (Aldrich, ≥99.95%), and Ag_2SO_4 (Sigma-Aldrich ≥99.5%). The chemicals were weighed individually followed by crushing and mixing them in a mortar. Glasses labelled Ag0 were melted in the furnace at 950°C for 5 minutes and Ag4 at 1050°C for 10 minutes. Ag0 glasses were melted in platinum crucible and Ag4 in alumina crucible. After quenching, the glasses were annealed at 200°C for 4 hours.

In order to prepare glass-ceramics, the Ag0 glass was heat treated at the glass transition temperature T_g+20°C (290°C) for 17 hours and then at 390°C for 1 hour (Nommeots-Nomm, et al., 2018). The Ag4 glass was heat treated at T_g+20°C (320°C) for 2 hours to grow Ag NPs as in (Ohja, Bogdan, Galatus, & Petit, 2020). Labels for these samples are given in the following table.

Table 1. Labels of the prepared samples

Amount of Ag_2O (in mol-%)	0	4
As-prepared	Ag0	Ag4
Heat-treated at T_g+20°C for 2 hours	-	Ag4 NP
Heat-treated at (T_g+20°C) for 17 hours and 390°C for 1 hour	Ag0 CR	-

3.2 Irradiation trials and laser setups

In this project the samples were irradiated using a CO_2 laser as well as a femtosecond (fs) laser. The irradiation with the CO_2 laser was done by the author at Tampere University in FabLab facilities. The fs laser experiments were performed in collaboration with

Dr. Maxime Cavillon at Université Paris-Saclay, France. All the samples were polished before irradiation.

3.2.1 CO_2 laser

The irradiation was done using an Epilog Laser Fusion M2 40 laser system provided by FabLab facilities. The system has a 75 W CO_2 laser. This system allows for the power and speed of the laser to be adjusted in 1% increments from 1 to 100 %.

To determine when ablation occurs when using the CO_2 laser, trials with different parameters were conducted. The results of these trials are discussed in chapter 4.2.1. Frequency of the laser was set to 100 Hz and the resolution was set to 600 dpi. The laser was focused manually, and the laser was moved during the writing while the stage stayed still.

Parameters for irradiation were selected according to the results of the ablation trials. A 1mm x 1mm square was drawn with 2mm long lines around it to mark the area, like illustrated in Figure 10.

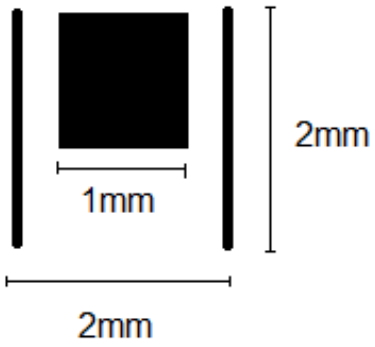

Figure 10. Illustration of square written at the surface of the glass surrounded by 2 ablated lines to mark the irradiation area.

The square was formed by drawing vertical and horizontal lines next to each other 0.1 mm apart. The square was the actual studied area and thus was irradiated with multiple different parameters that will be discussed in the next chapter. Longer lines were drawn with high power and slow speed to leave a visible mark. This was done to find the irradiated areas and thus ease the analysis process.

3.2.2 Fs laser

Samples were also irradiated with a fs laser (Satsuma, Amplitude Systèmes Ltd. Pessac, France) which has a wavelength of 1030 nm, pulse duration of 250 fs and numeric aperture of 0.6.

A schematic of the setup is presented in Figure 11, where S is scanning direction.

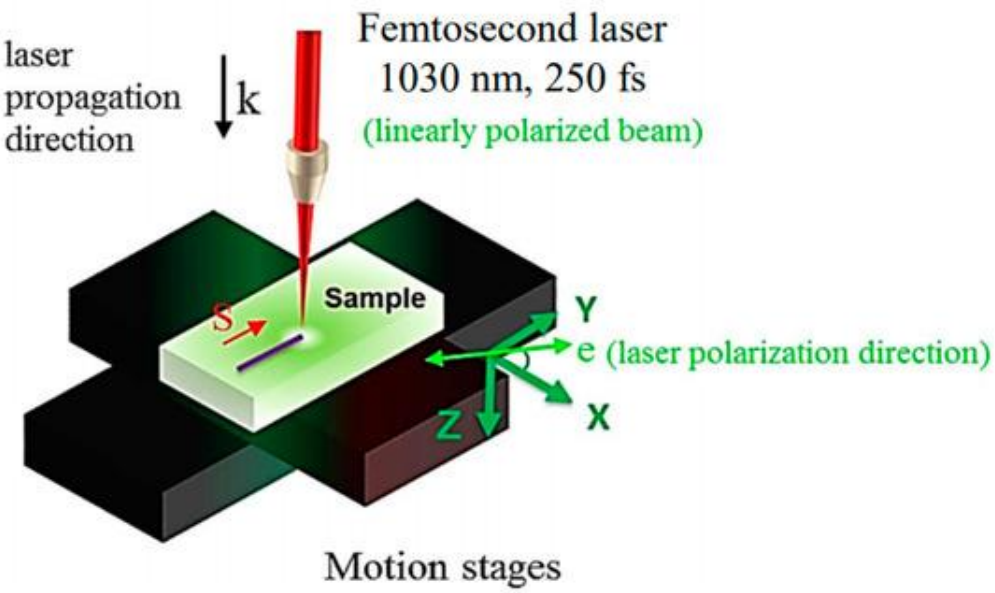

Figure 11. Schematic of the fs laser setup (Muzi, et al., 2021).

Ablation threshold trials for the fs laser were also conducted and the results are presented in chapter 4.3.1. Based on these trials it was chosen that the samples were irradiated using energies varying from 0.01 to 1 µJ with a 45° polarization. 100x30 µm rectangles were drawn in the manner that is shown in Figure 12.

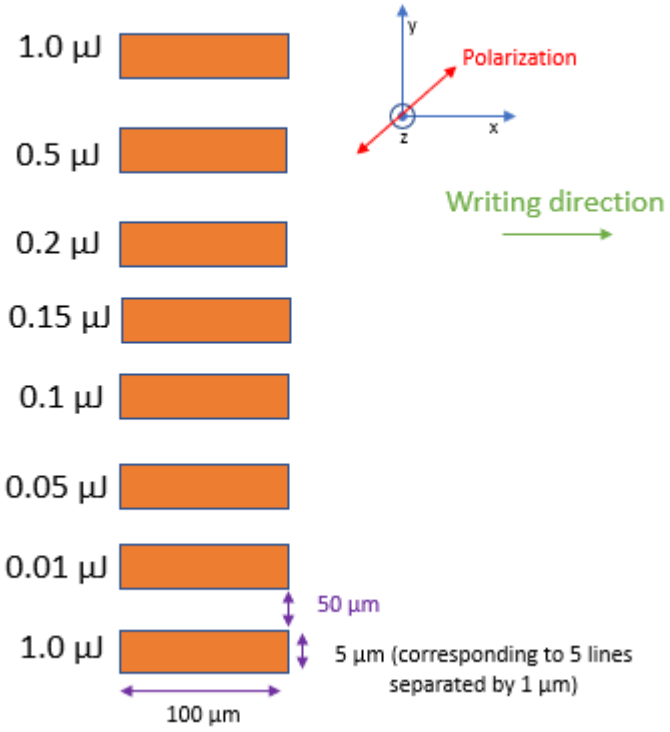

Figure 12. Illustration of the irradiation of the samples.

During the irradiation a repetition rate of 10 kHz was used, and the writing speed was 1 µm/s. All the samples were irradiated on the surface.

3.3 Profilometer

The surface profiles of the irradiated samples were measured using Veeco Wyko NT1100 surface profiler.

A schematic of the surface profiler can be found in Figure 13.

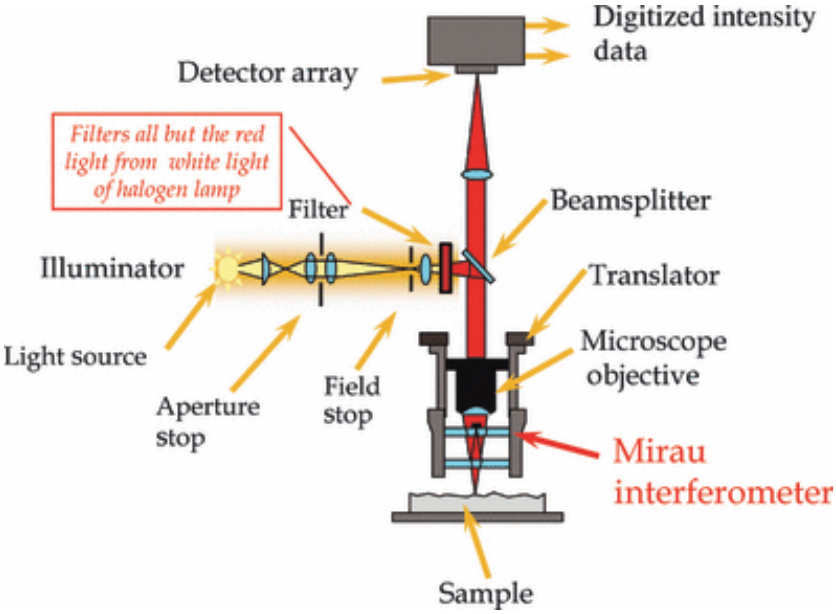

Figure 13. Schematic of the surface profiler. (Giraldez, García-Resúa, Lira, Real Oliveira, & Yebra-Pimentel, 2010)

The beam is focused on the surface of the sample. A backscan of 10 µm was used so that the measurement starts 10 µm above the focus point on the surface of the sample. The length of the measurement was 50 µm, which means that the measurement was stopped 50 µm below the focus point. The modulation threshold of the measurement helps to account for the roughness of the sample surface, by determining the acceptable signal-to-noise level. When measuring an extremely smooth and reflective sample like glass, a modulation threshold of 10% is usually used. For rougher samples, a lower modulation threshold would be preferred to avoid having too many data points excluded from the analysis. For the samples in this project a value of 5% was used as the surface of the samples was not perfectly polished and smooth. The Cylinder & tilt filter was used to remove the general shape of the surface and leave only the microstructure of the sample. To smooth the data, filtering was used: Median smoothing filter sorts the height values in the window in ascending order and the median is stored as the new centre height. This filter is effective in preserving edges and steps in the data.

A field-of-view lens of 0.5X and an objective of 5.0X were used. The system only allows for a maximum of 8.24 mm area to be imaged; therefore, the stitching mechanism of the system was used to measure larger areas. This allows for multiple measurements to be joined together to form a single picture. During stitching an objective of 2.5X was used.

3.4 Confocal Raman microscope

The structural and luminescence properties of the as-prepared and irradiated samples was investigated using Renishaw InVia Qontor confocal Raman microscope.

A schematic of the microscope is presented in Figure 14.

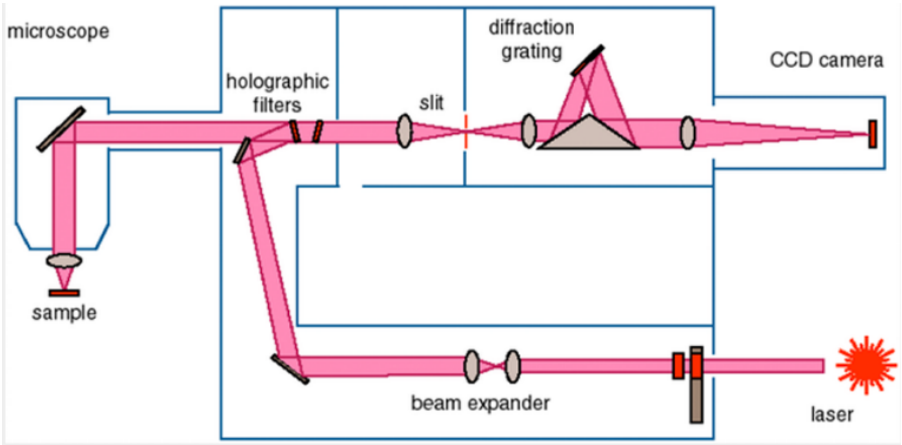

Figure 14. Schematic of the confocal Raman microscope. (University of Colorado, 2023)

This setup allows for both microraman and microluminescence spectra of the samples to be measured. The microscope is equipped with three different excitation lasers: 405, 532, and 785 nm. It has a wavelength range from 200 nm to 2200 nm.

3.4.1 Raman spectra

Raman spectroscopy is used to study the vibrational transitions of a material and so to get information about the structure of the glass. When a material is irradiated, its molecules scatter the light. In Raman spectroscopy, the irradiation is done with a laser that is in the UV-visible range and the light is scattered in two types: Rayleigh scattering and Raman scattering. Rayleigh scattering is strong and needs to be filtered out when measuring Raman scattering which in turn is very weak. Raman scattering has frequencies $v_0 \pm v_m$, where v_0 is the frequency of the incident beam and v_m is a molecules vibrational frequency and this shift is what is measured in Raman spectroscopy. This shift is represented in Figure 15 by means of energy level comparison. (Ferraro, Nakamoto, & Brown, 2003)

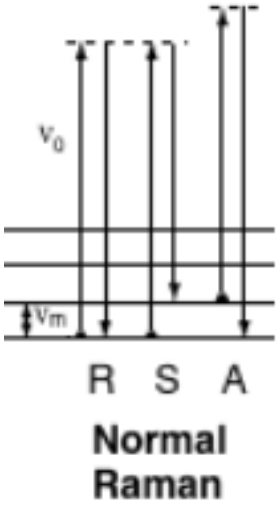

Figure 15. Energy levels for Raman spectra. R=Rayleigh, S=Stokes, A=anti-Stokes. Modified from (Ferraro, Nakamoto, & Brown, 2003)

Raman scattering can be divided into Stokes and anti-Stokes scattering which are both represented in the forementioned equation; the negative ν_m represents Stokes and the positive anti-Stokes scattering. These have the same values, but as can be seen from the example in Figure 16, the Stokes scattering has a higher intensity and thus usually only this side of the spectrum is measured. (Ferraro, Nakamoto, & Brown, 2003)

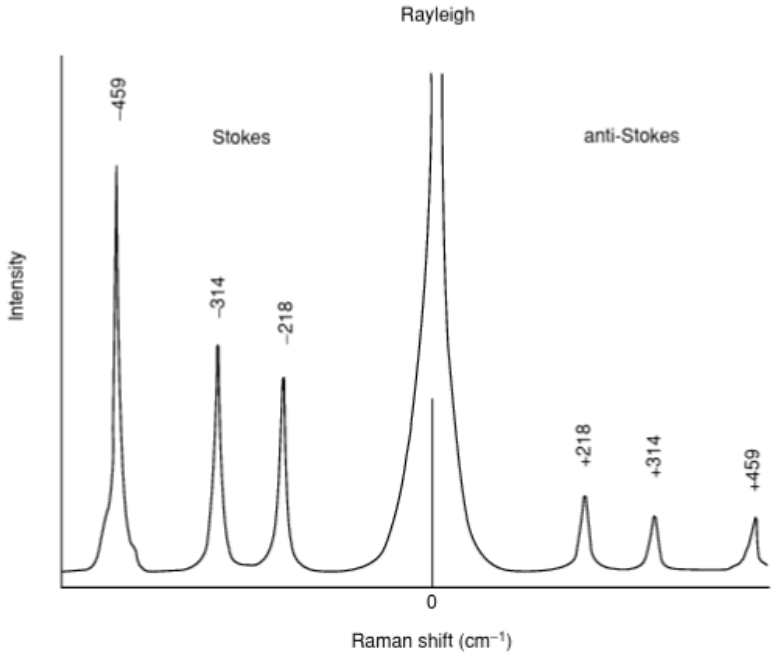

Figure 16. Raman spectrum of CCl_4. (Ferraro, Nakamoto, & Brown, 2003)

In this project, the Raman spectra were measured using an excitation wavelength of 785 nm and a grating of 1200. A power of 10% and measurement time of 30 seconds were chosen.

3.4.2 Emission spectra

Luminescence has been a phenomenon that has intrigued humans from the beginning of recorded history. It can be observed for example in glow worms, fireflies, some sea creatures such as jellyfish, various gemstones, and the aurora borealis aka the northern lights. (Demas & Demas, 2001) (Capelletti, 2005) The luminescence phenomenon was first studied on the Bolognian Phosphorus which was discovered in 1602 by Vincenzo Casciarolo (Capelletti, 2005). Luminescence studies how matter absorbs and emits radiation. It does not generate heat, nor does it require heat to occur which means that it happens in normal and cool temperatures. (Kalyani, Swart, & Dhoble, 2017) Light emitted in luminescence is in the ultraviolet, visible, or infrared range. The phenomenon is caused by the radiative transitions of electrons from an excited state to a lower energy level. (Demas & Demas, 2001)

There are multiple different types of luminescence, and they can be categorized by the way that the excitation of electrons is achieved.

- When electrons are excited by photons been absorbed by the matter the emission is called photoluminescence.
- Electric current through matter causes electroluminescence and cathodoluminescence.
- Chemiluminescence, or bioluminescence in biological systems, is caused by chemical reactions.
- Radioluminescence occurs when ionizing radiation or subatomic particles pass though matter.
- If sample is heated gently, thermoluminescence can occur.
- If the emission happens as the matter is irradiated that is called fluorescence and if the emission continues for some time after the excitation is ceased that is called phosphorescence or afterglow. (Capelletti, 2005)

The wavelength of the emitted light depends on the material (Kalyani, Swart, & Dhoble, 2017).

Rare-earth elements are particularly efficient in producing luminescence. Their 4f shells are not completely filled, but this shell is shielded from the host lattice by the completely

filled 5s and 5p shells which are on the outer side of the 4f shell. The radiative transitions responsible for luminescence in tripositive RE ions occur mainly in the 4f shell. Quantum mechanical spin and parity prohibition rules usually deem this forbidden, but luminescence can still be possible under the condition that these ions are not in the crystalline lattice's centre of symmetry position. Tripositive RE ions (such as Eu^{3+} and Tb^{3+}) are excellent luminescence emitters due to the number of electrons in their 4f shells. (Kalyani, Swart, & Dhoble, 2017)

The luminescence spectra for this project were measured using a 532 nm excitation wavelength and 2400 grating. A power of 0.5% and measurement time of 30 seconds were deemed adequate for these measurements.

4 RESULTS AND DISCUSSION

The goal of this project was to understand the glass-light interaction. In addition, there was an interest in trying out whether laser could be used to locally crystallize glass or amorphize glass-ceramic samples as well as locally form / dissolve silver nanoparticles in silver containing glass samples.

4.1 Characterization of the as-prepared glasses using confocal microscope

The oxyfluorophosphate glasses were heat treated in order to grow Ag NPs (NP) but also at higher temperature to precipitate CaF_2 crystals (CR).

The normalized microraman spectra of the investigated glass-based materials are presented in Figure 17.

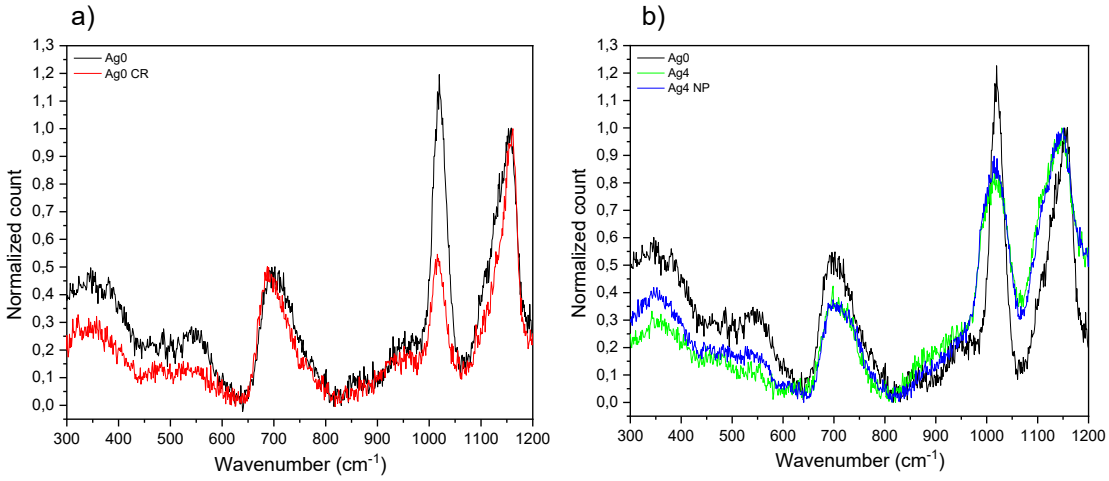

Figure 17. Normalized microraman spectra of nonirradiated (a) as prepared (Ag0) and heat treated (Ag0 CR) glasses without Ag and (b) as prepared (Ag4) and heat treated (Ag4 NP) Ag containing glasses. The excitations wavelength was 785 nm.

The Raman spectra exhibit few bands. The band at 700 cm^{-1} can be matched with the deformation modes of P-O-P bridges. The bands at 1020 and 1150 cm^{-1} are from the symmetric stretching of non-bridging P-O bonds in Q^1 and Q^2 tetrahedra respectively. The presence of these Raman bands indicates that the glass has a metaphosphate structure. The shoulder at around 950 cm^{-1} can be associated with the symmetric stretching of PO_4 on Q^0 tetrahedra. Bands in the 300-600 cm^{-1} range can be related to network

deformations caused by the Q^1 and Q^0 tetrahedra. (Brow, 2000) (Möncke & Eckert, 2019) There is a very small peak at 320 cm^{-1} in the spectrum of Ag0 CR which could be from CaF_2 crystallization (Kristalle, 2021) (Lewis, et al., 2017). Ag NPs are known to exhibit peaks at 470 and 627 cm^{-1} (Joshi, et al., 2018). However, these peaks are not visible in the Raman spectrum of the glass expected to have Ag NPs.

It is clearly shown here that,

- the heat treatment used to crystallize the glass leads to a decrease in intensity of the Raman bands in the 300-600 cm^{-1} range but also of the band at 1020 cm^{-1} when compared to the band at 1150 cm^{-1} indicating that the precipitation of CaF_2 leads to the transformation of some of the Q^1 tetrahedra into Q^2 tetrahedra.
- Addition of Ag_2O leads to a decrease in the intensity of the bands at 700 and 1020 cm^{-1}. This indicates that some of the Q^1 tetrahedra transform into Q^2 tetrahedra when adding Ag_2O.
- The heat treatment to form Ag NPs leads to a slight increase in the intensity of the bands in the range 300-600 cm^{-1}. This increase is result of the deformation of the network caused by the Q^1 and Q^0 tetrahedra.

Figure 18 show the emission spectra of the glasses.

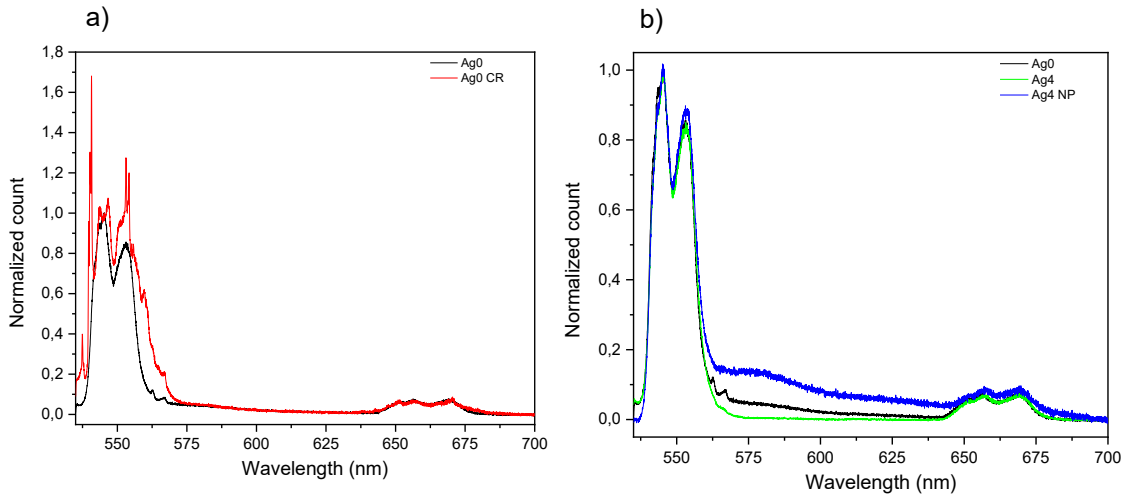

Figure 18. Normalized microluminescence spectra of nonirradiated (a) Ag0 and Ag0 CR and (b) Ag4 and Ag4 NP glasses. The excitation wavelength was 532 nm.

The emission spectra show the typical green and red emissions from Er^{3+} ions which are due to $^2H_{11/2}$,$^4S_{3/2} \rightarrow {}^4I_{15/2}$ and $^4F_{9/2} \rightarrow {}^4I_{15/2}$ transitions, respectively (Liang, Huang, & Zhang, 2009).

- The crystallization can be evidenced by the appearance of sharp peaks in the 525-575 nm range in the emission spectrum.
- The addition of Ag2O has no noticeable impact on the emission spectrum of the glass.
- The heat treatment to form Ag NPs leads to the appearance of a broad emission band at ~580 nm which is suspected be related to Ag NPs formation (Parang, et al., 2012) and/or phosphorus-oxygen hole centre (POHC) defect (Fletcher L. , et al., 2011).

4.2 Irradiation with CO_2 laser

4.2.1 Ablation threshold

Prior to investigate the photo-response of the glass, it is crucial to determine the maximum power and speed to use before ablating the glass (ablation threshold). Glasses were irradiated using speeds between 10-100 % with and interval of 10 % and power of 1-8 % with an interval of 1 %. After irradiation, the surface profile of the samples were measured to confirm whether ablation has occurred or not. Figure 19 shows the pictures of the surface profiles of the irradiated Ag4 glass, taken as an ex-ample.

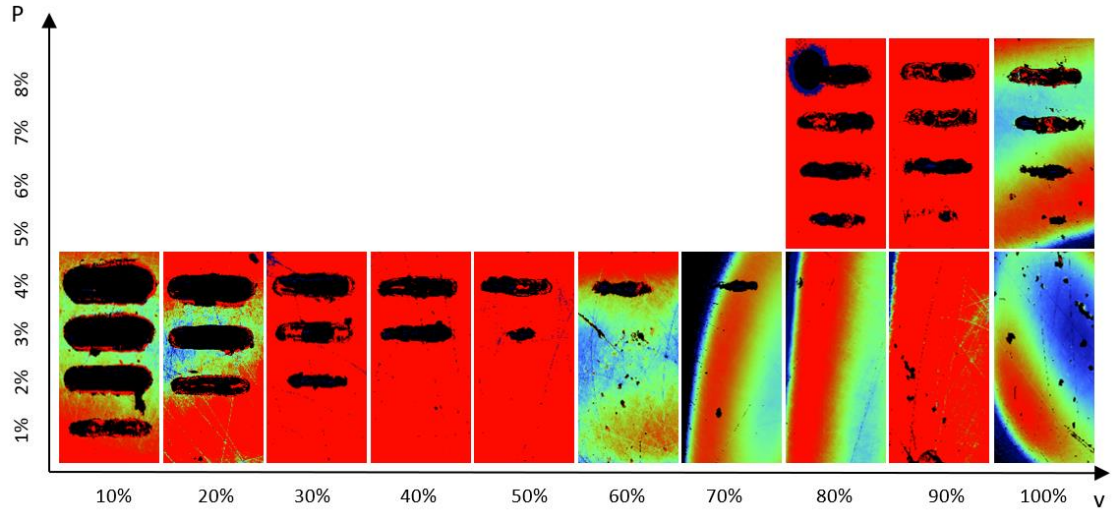

Figure 19. Pictures of the surface profiles of the irradiated Ag4 samples as a function of power (P) and speed (v) (length of the line is 2 mm).

In these pictures, the black colour means there is no data, because the hole is too deep for the measurement to reach the bottom. This is also a clear indicator of ablation. An increase in power and decrease in speed leads to ablation. No dark lines are observed when using speed larger than 80%. With the lowest power (1 %), the lowest speed that

did not cause ablation was 30 %. Every power above 4 % causes ablation at all speeds. When using 4 % power, 90 % speed does not cause ablation.

For more accurate analysis, the surface profiles were measured. Figure 20 depicts is an example of one of the surface profiles confirming the ablation.

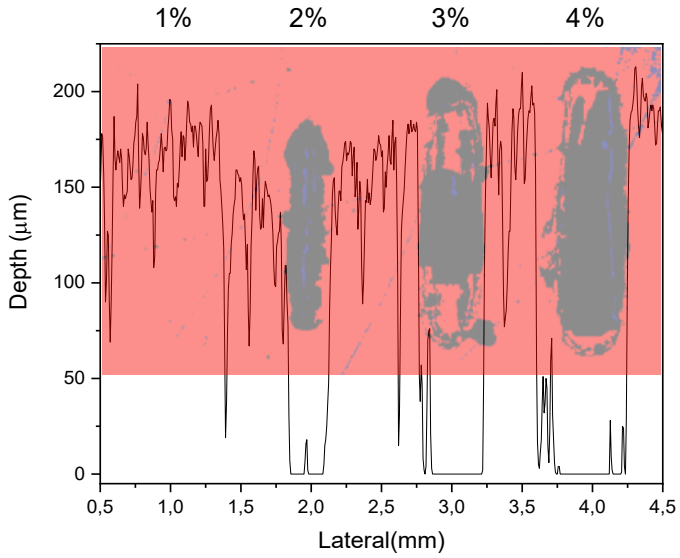

Figure 20. Surface profile of the Ag4 glass that was irradiated with 1-4 % power and 30 % speed.

The surface profile example clearly shows ablation when irradiating the glass with 2-4 % power and no ablation is observed when using 1 % power.

4.2.2 Photoresponse

Based on Figure 19, the samples were irradiated using 1 % power and 30 % speed as well as 4 % power and 90 % speed, parameters suspected to be the highest power and slowest speed before getting ablation. The samples were irradiated using one pass of the laser as well as 50 passes in order to increase locally the heat. In addition to this, parameters that cause ablation were chosen to mark the irradiation site for easier analysis; 3 % power and 40 % speed.

To make the discussion of these parameters simpler, code names for them are provided in Table 2.

Table 2. Parameters of the irradiation zones in samples irradiated with CO_2-laser.

Irradiation zones	Power	Speed	Passes
Ablation	3 %	40 %	1
1-30(1)	1 %	30 %	1
1-30(50)	1 %	30 %	50
4-90(1)	4 %	90 %	1
4-90(50)	4 %	90 %	50

Surface profile

The 3D surface profile of the Ag0, Ag0 CR, Ag4 and Ag4 NP glasses after irradiation is shown in Figure 21.

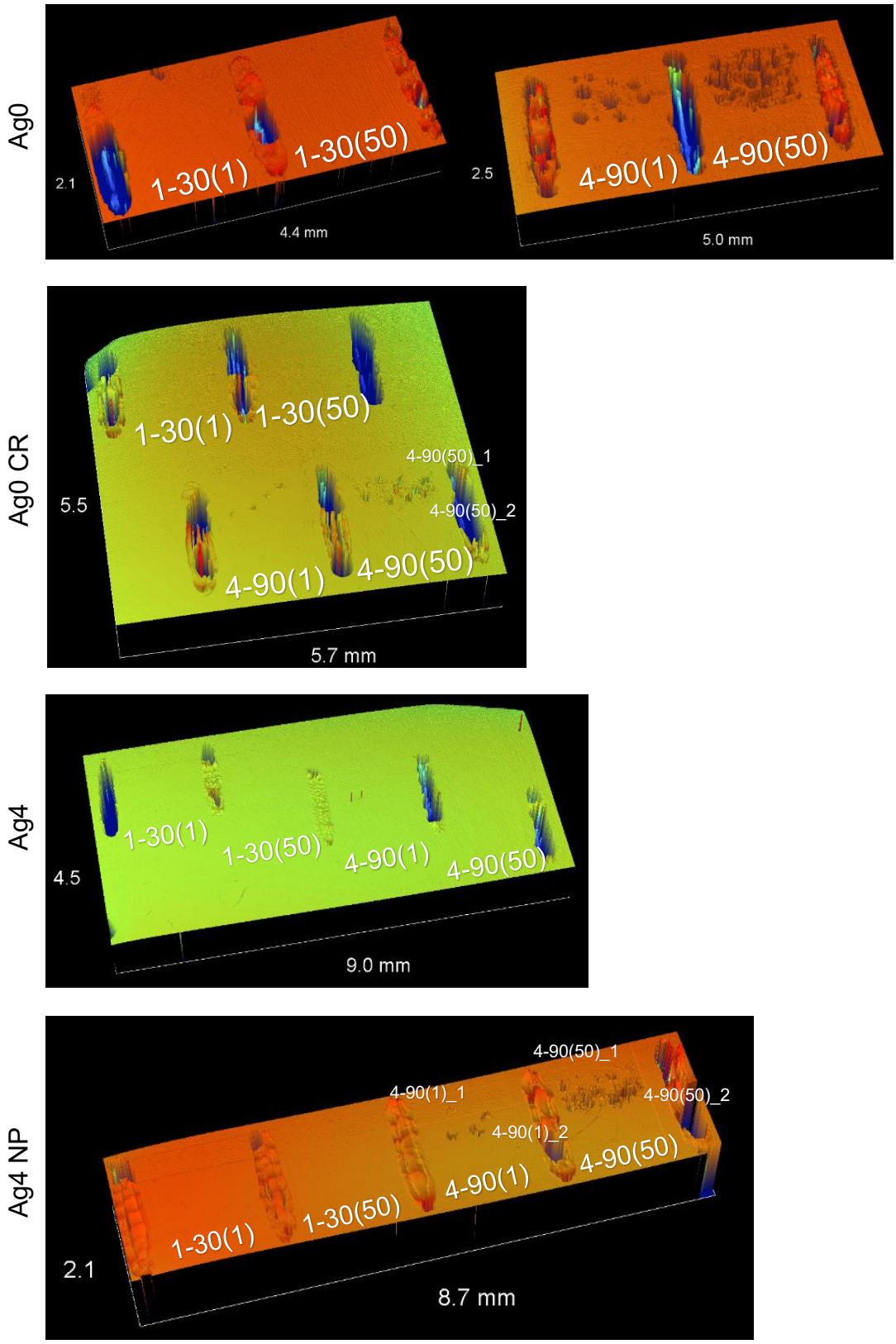

Figure 21. 3D picture of the surface of Ag0, Ag0 CR, Ag4 and Ag4 NP glasses after irradiation using 1 to 4 % power, 30 to 90 % speed and 1 or 50 passes.

For all the glasses, the areas irradiated with 1 % power and 30 % speed do not show signs of ablation which was expected according to Figures 19 and Figure 20. However, some samples exhibit ablation after irradiation with 4 % power and 90 % speed.

- Less surface damage is observed after crystallizing the glass indicating that the precipitation of the CaF_2 crystals in the glass can be used to increase the photo-resistance of the glass.
- The addition of Ag_2O seems to also increase the photo-resistance of the glass as no surface damage was observed.
- Some surface damage can be seen in the glass prepared with Ag NPs indicating that the Ag4 glass is more sensitive to laser irradiation when Ag are agglomerated into NPs.

These observations should be analysed carefully as they depend strongly on the sample preparation: issue with parallelism would change the focus point of the laser at the surface of the sample and so the power on the surface of the sample. Nonetheless, the presence of crystals (CaF_2 in this study) is used to increase glass toughness by limiting the formation and propagation of the microcrack (Inage, et al., 2020). It is therefore possible to expect that the heat treatment can be used to increase the photoresponse of the glass. It appears that a glass with polymerized network with large amount of Q^2 units is less sensitive to laser irradiation than a glass with depolymerized network.

Structural properties

The microraman spectra were measured in the irradiated and non-irradiated (NI) areas and they are presented in Figure 22.

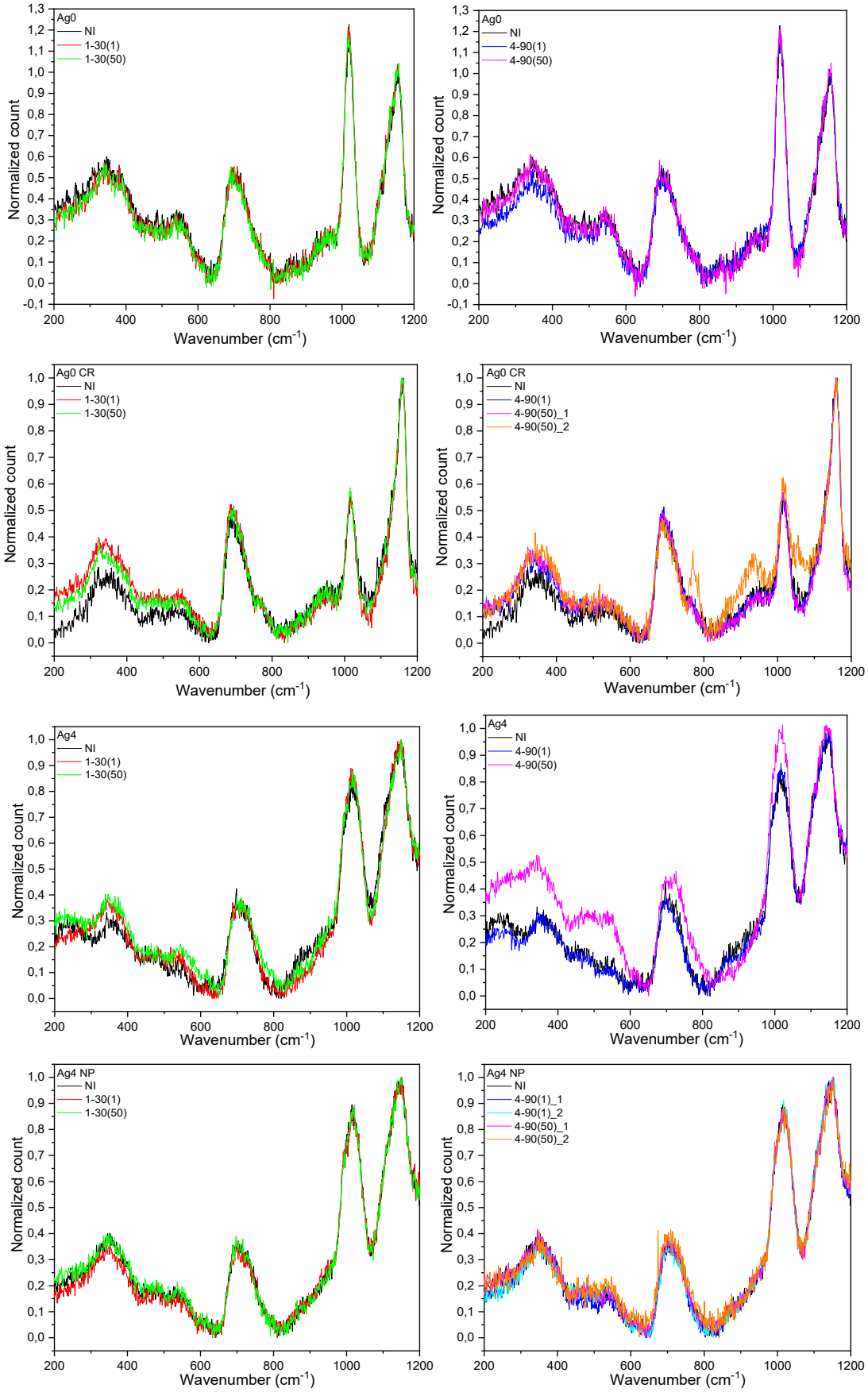

Figure 22. Normalized microraman spectra of Ag0, Ag0 CR, Ag4 and Ag4 NP glass after irradiation using 1 to 4 % power, 30 to 90 % speed and 1 or 50 passes. The excitations wavelength was 785 nm.

Despite visible ablation on the surface (Figure 21), the Ag0 glass shows no significant changes in its Raman spectrum after irradiation indicating that the irradiation did not induce significant changes in the structure of the glass nor crystallization. No shift in the position of the bands was observed either which is in agreement with the surface profile as no expansion nor contraction was observed (Fletcher L. , et al., 2011).

On the other hand, the Ag0 CR exhibits a slight increase in the intensity of the band in 200-600 cm^{-1} range and of the band at 700 cm^{-1} after irradiation indicating some network deformations occurring during laser irradiation. However, these changes do not provide the evidence of amorphization of the crystallized glass during the radiation treatment. Ag0 CR glass was measured in an ablated area (4-90(50)_2 (orange)) and this spectrum shows new peaks at around 760, 950, and 1060 cm^{-1}. The peak at 950 cm^{-1} can be associated with the symmetric stretching of PO_4 on Q^0 tetrahedra. The peaks at 760 and 1060 cm^{-1} are characteristic to pyrophosphate polycrystalline glasses (Anastasopoulou, et al., 2017). These changes in the Raman spectrum clearly show significant changes in the structure of the glass in the ablated area. It is possible to think that the radiation treatment leads to the growth of the CaF_2 crystals. This assumption needs to be confirmed using SEM for example.

The irradiation of the Ag4 leads to modification in the Raman spectra: increase in intensity of the band in the 200-600 cm^{-1} range which might indicate changes in the glass structure but also might be a sign for Ag NPs formation. There is also an increase in the bad at 700 cm^{-1} and 1020 cm^{-1}. This indicates that some of the Q^2 tetrahedra transform into Q^1 tetrahedra. Surprisingly, no changes in the Raman spectra of the Ag4 NP can be noticed after irradiation although this glass is suspected to be more photosensitive than the Ag4 glass as discussed in the previous paragraph. This suggests that the Ag NPs do not dissolve back in the glass during the irradiation.

Spectroscopic properties

The normalized microluminescence spectra of the irradiated and non-irradiated (NI) areas are presented in Figure 23.

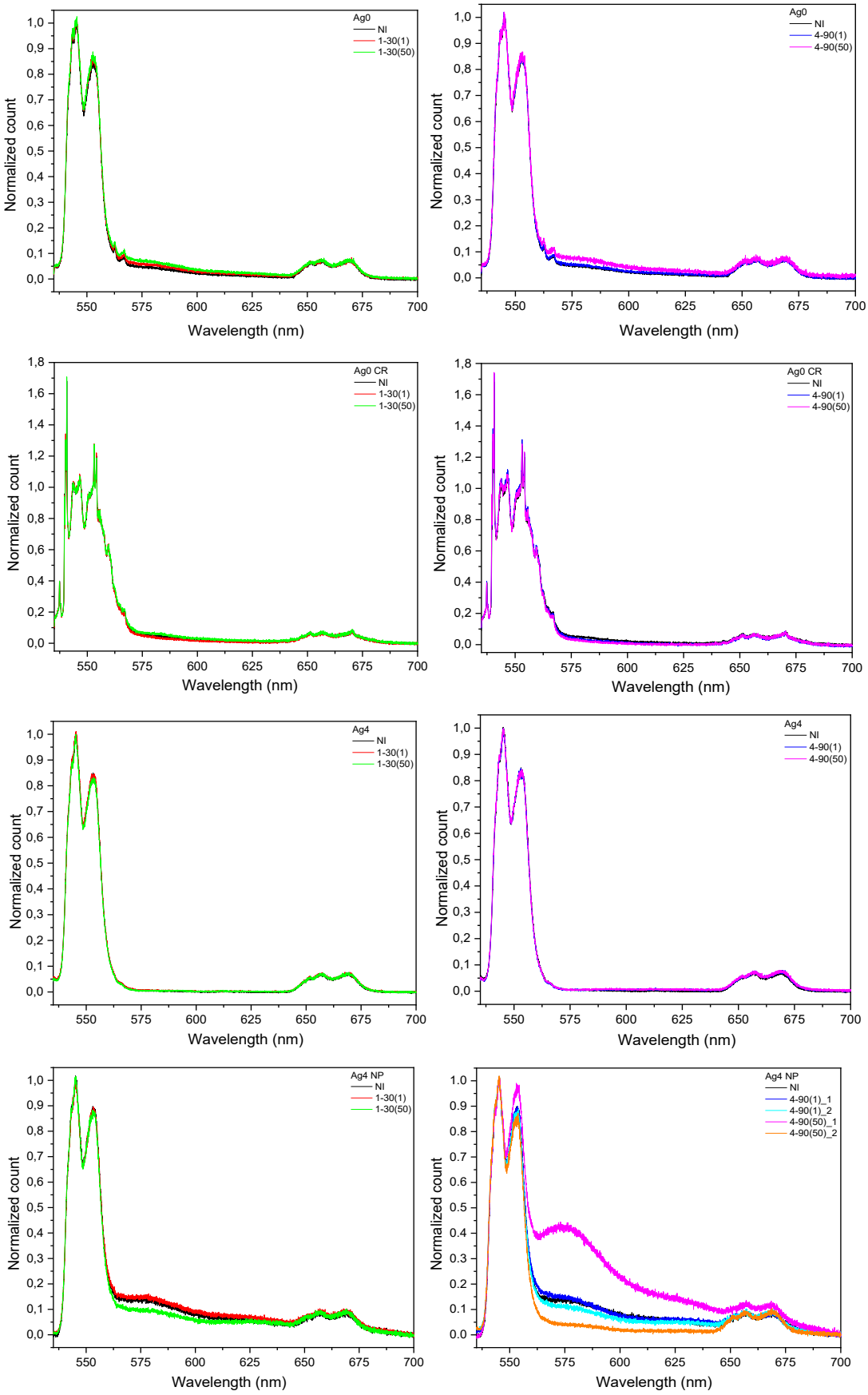

Figure 23. Normalized microluminescence spectra of Ag0, Ag0 CR, Ag4 and Ag4 NP glasses after irradiation using 1 to 4 % power, 30 to 90 % speed and 1 or 50 passes. The excitation wavelength was 532 nm.

No noticeable changes in the emission spectrum of the Ag0 and Ag0 CR can be observed after irradiation indicating that the irradiation has no impact on Er^{3+} sites in glass and crystallized glass. No crystallization nor amorphization is expected to occur during the radiation treatment. However, a slight increase in intensity of the shoulder at 575 nm can be seen when using high power and multiple passes. The appearance of this new band is likely due to the POHC defect formation as a result of heat from the irradiation (Fletcher L. , et al., 2011).

Whereas the emission spectra remain unchanged after irradiating the Ag4 glass, the Ag4 NP shows drastic changes, especially with the appearance of the band ~580 nm, the intensity of which increases with increase in power and number of passes. This might indicate the formation of POHC defects in this glass and/or more Ag NPs. However, if ablation occurred (orange spectrum), the Ag NPs might dissolve during the irradiation.

In order to confirm the defect formation in irradiated glasses, the emission spectra were also recorded on the ablated lines used to mark the irradiation sites and the spectra are presented in Figure 24.

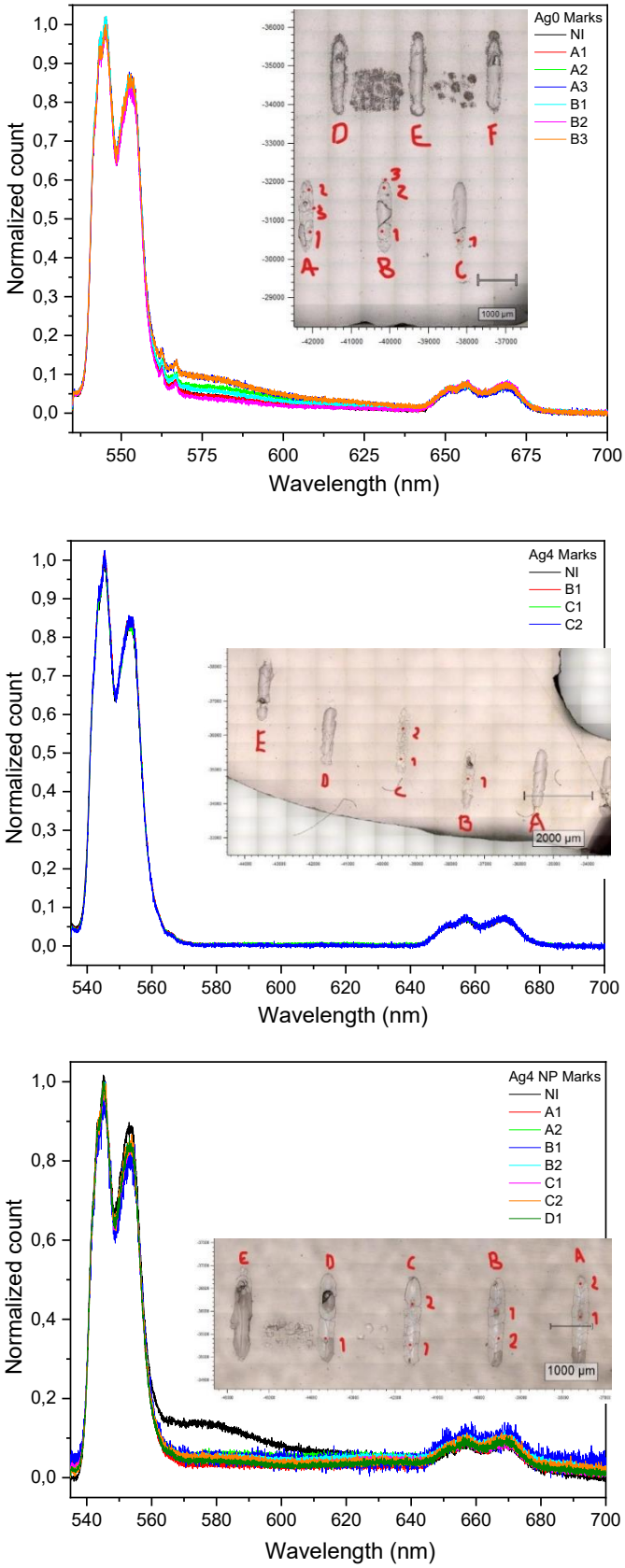

Figure 24. Normalized microluminescence spectra of Ag4 NP marks after irradiation using 3 % power, 40 % speed and 1 pass and information on the locations of irradiation. Information picture upside-down compared to 3D surface profile. The excitation wavelength was 532 nm.

When measured on the ablated lines

- the increase in intensity of the shoulder at 580 nm after irradiation might indicate the formation of defects in Ag0. However, the emission spectra of the Ag4 glass remain unchanged after irradiation confirming that the Ag4 glass is more photo-resistant probably due to its polymerized network compared to Ag0.
- a decrease in the intensity of the emission at 580 nm is seen in the spectrum of the Ag4 NP after irradiation suggesting that the defects and/or NPs are dissolved during the radiation treatment using high power, slow speed.

4.3 Irradiation with fs laser – Preliminary results

This work was performed in collaboration with Dr. Maxime Cavillon at Université Paris-Saclay, France using Satsuma, Amplitude Systèmes laser.

4.3.1 Ablation threshold

The ablation threshold was estimated using the femtosecond laser (the Ag4 NP glass is still to be irradiated). The translation speed was 1µm/s. Repetition rate was varied from 10 to 100kHz and the pulse energy from 0.01 to 1 µJ. The pictures of the sample surface after irradiation are shown below.

a)

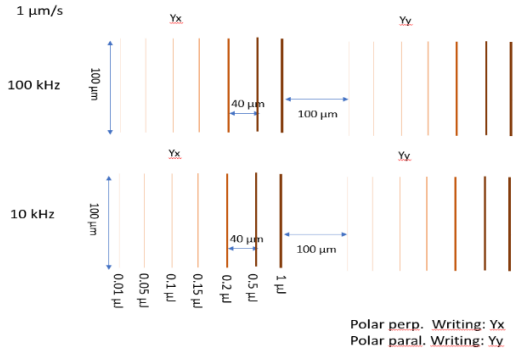

b) Ag0 CR

c) Ag4

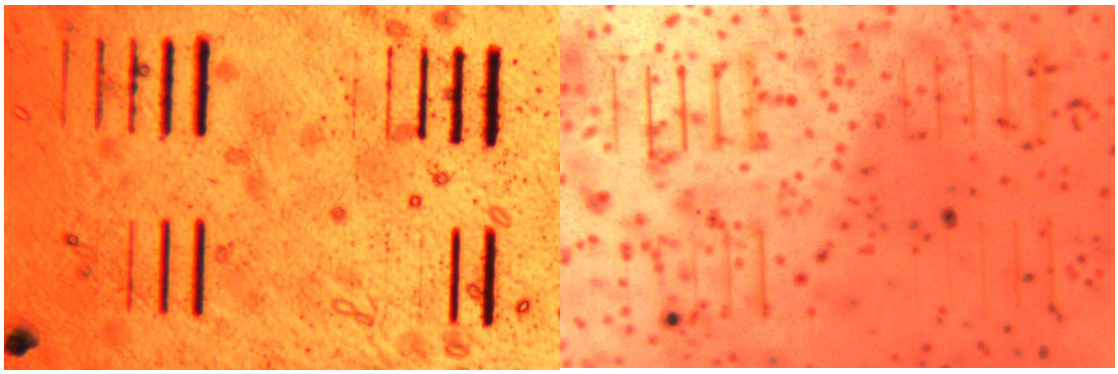

Figure 25. Pictures of the irradiation tests (b, c) performed with the femtosecond laser. a) shows the information of the irradiation parameters used.

As seen in Figure 25, the frequency of 10 kHz and low pulse energy seemed to cause the least ablation. Ag0 was irradiated but no lines could be seen whereas lines can be easily found at the surface of the Ag0 CR (lines seen in Figure 25b) and Ag4 (lines seen in Figure 25c) suggesting that the photoresponse of the glass can be increased using thermal treatment and/or by adding Ag_2O. The crystallized glass seems to be the most sensitive to laser irradiation. Different laser parameters are thus needed for the irradiation of the Ag0 glass.

4.3.2 Photoresponse

The samples were irradiated on the surface using energies varying from 0.01 to 1 µJ with 45° polarization, repetition rate of 10 kHz and the writing speed was 1 µm/s. The fs laser has a wavelength of 1030 nm, pulse duration of 250 fs and numeric aperture of 0.6.

A microscope picture of the transmission of the irradiated Ag4 glass is presented in Figure 26.

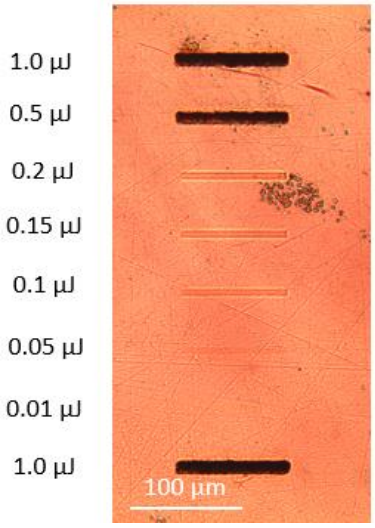

Figure 26. Microscope picture of the transmission of Ag4 glass irradiated with fs laser.

Most of the irradiated lines are visible. The lines irradiated with 1.0 and 0.5 µJ are clearly visible and line from 0.2 to 0.05 µJ are fainter but still can be detected whereas 0.01 µJ line cannot be seen.

To study if the irradiation caused contraction, expansion or ablation the surface profile of the irradiated area was measured, and it is presented in Figure 27.

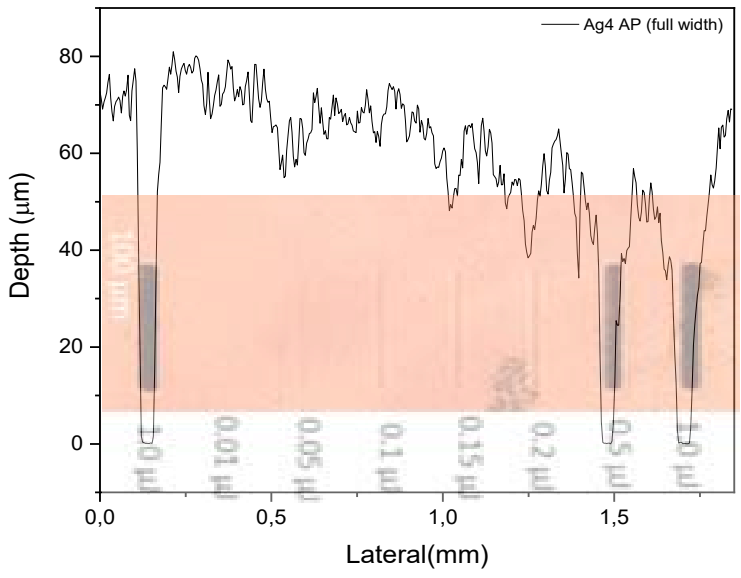

Figure 27. Surface profile of Ag4 glass irradiated with fs laser.

The lines made with 1.0 and 0.5 μJ pulse energies are severely ablated and 0.2 and 0.15 μJ have small amounts of ablation. The rest of the lines are not ablated but show some small changes that could indicate contraction of the glass network. This would be in agreement with the work by Fletcher, et al who reported surface contraction in Er – Yb codoped phosphate glass under femtosecond laser irradiation (Fletcher L. , et al., 2009).

Attempts to measure the microraman and microluminescence spectra of the glasses prior to and after irradiation were performed but no detectable signal could be obtained indicating that the lines are probably written sub-surface.

5 CONCLUSION

In this project, Er^{3+} doped phosphate glasses were prepared with and without silver. The glasses with composition (100 – 0.25 – x) (75 $NaPO_3$ – 25 CaF_2) – 0.25 Er_2O_3 – x Ag_2O, where x=0 or x=4 in mol-% (labelled Ag0 and Ag4 respectively), were heat-treated at T_g+20°C for 17 hours and 390°C for 1 hour to form CaF_2 crystallization and at T_g+20°C for 2 hours to form Ag nanoparticles. Heat treated samples were labelled Ag0 CR and Ag4 NP respectively. The formation of CaF_2 crystals was confirmed from the sharp peaks in the emission spectrum measured from the heat-treated glass. The precipitation of Ag NPs in the heat treated Ag4 glass can also be suspected from the increase in the intensity of the emission band at ~580 nm.

Glasses were irradiated using CO_2 and fs lasers. First irradiation trials were conducted to determine the ablation threshold of the samples. From these results the irradiation parameters were selected to not cause ablation on the glass surface. A surface profiler was used to study whether ablation has occurred. CO_2 laser was used to irradiate all prepared glasses with two sets of parameters; 1 % power & 30 % speed and 4 % power & 90 % speed. Both sets of parameters were used to irradiate using 1 and 50 passes. Surface profile measurements of all the glasses irradiated with CO_2 laser indicate that neither expansion nor contraction of the glass network occurs. Crystallization and addition of Ag_2O seem to decrease the photosensitivity of the glasses as Ag0 CR and Ag4 glasses have much less ablation than the Ag0 glass. The agglomeration of Ag NPs however makes the glass more photosensitive. The irradiation is expected to cause the precipitation of phosphorus-oxygen hole centre (POHC) defects. However, the irradiation does not induce crystallization nor amorphization in the glasses without silver. In the silver containing glasses, the irradiation cannot be used to form Ag NPs, but when the glass was heat treated beforehand, the laser could be used to further grow Ag NPs using high laser power and multiple passes. However, when ablation occurred, the NPs formed by the heat treatment can be dissolved.

Fs laser was used to irradiate the glasses. The glasses were irradiated using pulse energies ranging from 0.01 to 1 µJ, 10kHz repetition rate, 1 µm/s writing speed and 45° polarization. Although irradiated, the Ag0 glass did not show any signs of the irradiation. Ag4 glass irradiated with fs laser shows indications of surface contraction when irradiated with low pulse energies.

Overall, the irradiation is a difficult process especially because the glasses were home-made and not polished perfectly. This led to issues with the laser power staying consistent in different parts of the glass surface as the focus point was not consistently on the surface.

In future studies the glass preparation should be improved to avoid these complications. The glasses should be prepared with parallel surfaces. SEM could also be used to study the surface of the irradiated glasses, but its use is limited if the crystals are too small.

REFERENCES

Ams, M., Marshall, G., Dekker, P., Dubov, M., Mezentsev, V., Bennion, I., & Withford, M. (2008). Investigation of ultrafast laser–photonic material interactions: challenges for directly written glass photonics. *IEEE Journal of Selected Topics in Quantum Electronics, 14*(5), 1370-1381.

Anastasopoulou, M., Vasilopoulos, K. C., Anagnostopoulos, D., Koutselas, I., Papayannis, D. K., & Karakassides, M. A. (2017). Structural and Theoretical Study of Strontium Borophosphate Glasses Using Raman Spectroscopy and ab Initio Molecular Orbital Method. *Journal of Physical Chemistry B, 121*(17), 4610-4619.

Andreeta, M. R., Cunha, L. S., Vales, L. F., Caraschi, L. C., & Jasinevicius, R. G. (2011). Bidimensional codes recorded on an oxide glass surface using a continuous wave CO_2 laser. *Journal of Micromechanics and Microengineering, 21*(2).

Bhardwaj, V. R., Simova, E., Corkum, P. B., Rayner, D. M., Hnatovsky, C., Taylor, R. S., Schreder, B., Kluge, M. (2005). Femtosecond laser-induced refractive index modification in multicomponent glasses. *Journal of Applied Physics, 97*(8).

Blackman, J. (2009). *Metallic Nanoparticles* (1st ed.). Amsterdam: Elsevier.

Brierre, R. (2009). *Wikimedia commons*. Retrieved 07 17, 2023, from https://commons.wikimedia.org/wiki/File:Laser_CO2.png

Brow, R. (2000). Review: the structure of simple phosphate glasses. *Journal of Non-Crystalline Solids, 263-264*, 1-28.

Capelletti, R. (2005). Luminescence. In F. Bassani, G. Liedl, & P. Wyder (Eds.), *Encyclopedia of Condensed Matter Physics* (pp. 178-189). Parma: Elsevier Ltd.

Chan, J. W., Huser, T. R., Risbud, S. H., Hayden, J. S., & Krol, D. M. (2003). Waveguide fabrication in phosphate glasses using femtosecond laser pulses. *Applied Physics Letters, 82*(15), 2371-2373.

Chan, J. W., Huser, T., Risbud, S., & Krol, D. M. (2001). Structural changes in fused silica after exposure to focused femtosecond laser pulses. *Optics Letters, 26*(21), 1726-1728.

Choi, J. (2009). Femtosecond Laser Written Volumetric Diffractive Optical Elements And Their Applications. Orlando, Florida: University of Central Florida.

Das, R., Phadke, P., Khichar, N., & Chawla, S. (2014). Plasmonic enhancement of dual mode fluorescence in a silver nano-antenna–ZnO:Er^{3+} hybrid nanostructure. *Journal of Materials Chemistry C, 2*(42), 8880-8885.

Demas, J., & Demas, S. (2001). Luminescence. In R. Meyers (Ed.), *Encyclopedia of Physical Science and Technology* (pp. 799-823). Virginia: Elsevier Science Ltd.

Dubov, M., Mezentsev, V., Manshina, A. A., Sokolov, I. A., Povolotskiy, A. V., & Petrov, Y. V. (2014). Waveguide fabrication in lithium-niobo-phosphate glasses by high repetition rate femtosecond laser: route to non-equilibrium material's states. *Optical Materials Express, 4*(6), 1197-1206.

Fernandez, T., Hernandez, M., Sotillo, B., Eaton, S., Jose, G., Osellame, R., Jha, A., Fernandez, P., Solis, J. (2014). Role of ion migrations in ultrafast laser written tellurite glass waveguides. *Opt. Express, 22*, 15298.

Ferraro, J. R., Nakamoto, K., & Brown, C. W. (2003). *Introductory Raman Spectroscopy* (2nd ed.). San Diego: Elsevier Science.

Fletcher, L., Witcher, J., Reichman, W., Arai, A., Bovatsek, J., & D.M., K. (2009). Changes to the network structure of Er-Yb doped phosphate glass induced by femtosecond laser pulses. *Journal of Applied Physics, 106*(8).

Fletcher, L., Witcher, J., Troy, N., Reis, S., Brow, R., & Krol, D. (2011). Direct femtosecond laser waveguide writing inside zinc phosphate glass. *Opt. Express, 19*(9), 7929-7936.

Giraldez, M. J., García-Resúa, C., Lira, M., Real Oliveira, M. C., & Yebra-Pimentel, E. (2010). White light interferometry to characterize the hydrogel contact lens surface. *Ophthalmic and Physiological Optics, 30*(3), 289-297.

Gonçalves, M., Santos, L., & Almeida, R. (2002). Rare-earth-doped transparent glass ceramics. *C. R. Chimie, 5*, 845-854.

Harilal, S. S., Freeman, J. R., Diwakar, P. K., & Hassanein, A. (2014). Femtosecond Laser Ablation: Fundamentals And Applications. In S. Musazzi, & U. Perini (Eds.), *Laser-Induced Breakdown Spectroscopy. Springer Series in Optical Sciences, vol 182.* (pp. 143-166). Berlin Heidelberg: Springer-Verlag. doi:10.1007/978-3-642-45085-3_6

Hofmeister, H., Thiel, S., Dubiel, M., & Schurig, E. (1997). Synthesis of nanosized silver particles in ion-exchanged glass by electron beam irradiation. *Applied Physics Letters, 70*(13), 1694-1696.

Höland, W., & Beall, G. H. (2019). *Glass-Ceramic Technology* (3rd ed.). Hoboken, New Jersey: John Wiley & Sons, Inc.

Hongisto, M., Veber, A., Petit, Y., Cardinal, T., Danto, S., Jubera, V., & Petit, L. (2020). Radiation-Induced Defects and Effects in Germanate and Tellurite Glasses. *Materials, 13*(17), 3846.

Inage, K., Akatsuka, K., Iwasaki, K., Nakanishi, T., Maeda, K., & Yasumori, A. (2020). Effect of crystallinity and microstructure on mechanical properties of CaO-Al_2O_3-SiO_2 glass toughened by precipitation of hexagonal $CaAl_2Si_2O_8$ crystals. *Journal of Non-Crystalline Solids, 534*, 119948.

Joshi, N., Jain, N., Pathak, A., Singh, J., Prasad, R., & Upadhyaya, C. P. (2018). Biosynthesis of silver nanoparticles using Carissa carandas berries and its potential antibacterial activities. *Journal of Sol-Gel Science and Technology, 86*, 682-689.

Kalyani, N., Swart, H., & Dhoble, S. (2017). *Principles and Applications of Organic Light Emitting Diodes (OLEDs).* Elsevier.

Karabulut, M., Melnik, E., Stefan, R., Marasinghe, G. K., Ray, C. S., Kurkjian, C. R., & Day, D. E. (2001). Mechanical and structural properties of phosphate glasses. *journal of Non-Crystalline Solids, 288*, 8-17.

Kassab, L. R., da Silva, D. S., & de Araújo, C. B. (2010). Influence of metallic nanoparticles on electric-dipole and magnetic-dipole transitions of Eu^{3+} doped germanate glasses. *Journal of Applied Physics, 107*(11), 113506. doi:10.1063/1.3431347

Kristalle, K. (2021). *Calcium Fluoride / RAMAN*. Retrieved 10 18, 2023, from https://www.korth.de/en/materials/detail/Calcium%20Fluoride%20/%20RAMAN

Laser Focus World. (2016). *Gas Lasers: CO_2 lasers - progressing from a varied past to an application-specific future*. Retrieved Heinäkuu 15, 2023, from https://www.laserfocusworld.com/lasers-sources/article/16546914/gas-lasers-co2-lasers-progressing-from-a-varied-past-to-an-applicationspecific-future

Lewis, A. T., Gaifulina, R., Isabelle, M., Dorney, J., Woods, M. L., Lloyd, G. R., Lau, K., Rodriguez-Justo, M., Kendall, C., Stone, N., Thomas, G. M. (2017). Mirrored stainless steel substrate provides improved signal for Raman spectroscopy of tissue and cells. *Journal of Raman Spectroscopy, 48*(1), 1-142.

Liang, X. F., Huang, X. Y., & Zhang, Q. Y. (2009). $Gd_2(MoO_4)_3:Er^{3+}$ Nanophosphors for an Enhancement of Silicon Solar-Cell Near-Infrared Response. *J Fluoresc, 19*, 285-289.

Mahraz, Z. A., Sahar, M. R., Ghoshal, S. K., Dousti, M. R., & Amjad, R. J. (2013). Silver nanoparticles enhanced luminescence of Er^{3+} ions in boro-tellurite glasses. *Materials Letters, 112*, 136-138.

Marquestaut, N., Petit, Y., Royon, P., Mounaix, P., Cardinal, T., & Canioni, L. (2014). Three-Dimensional Silver Nanoparticle Formation Using Femtosecond Laser Irradiation in Phosphate Glasses: Analogy with Photography. *Advanced Functional Materials, 24*(37), 5824-5832.

Mody, V. V., Siwale, R., Singh, A., & Mody, H. R. (2010). Introduction to metallic nanoparticles. *Journal of Pharmacy and Bioallied Sciences, 2*(4), 282-289.

Möncke, D., & Eckert, H. (2019). Review on the structural analysis of fluoride-phosphate and fluoro-phosphate glasses. *Journal of Non-Crystalline Solids: X, 3*, 100026.

Möncke, D., Reibstein, S., Schumacher, D., & Wondraczek, L. (2014). Irradiation-induced defects in ionic sulfophosphate glasses. *Journal of Non-Crystalline Solids, 383*, 33-37.

Moore, L. A., & Smith, M. C. (2022). Fused silica as an optical material. *Optical Materials Express, 12*(8), 3043-3059.

Muzi, E., Cavillon, M., Launcry, M., Brisset, F., Que, R., Pugliese, D., Janner, D., Poumellec, B. (2021). Towards a Rationalization of Ultrafast Laser-Induced Crystallization in Lithium Niobium Borosilicate Glasses: The Key Role of the Scanning Speed. *Crystals, 11*(3), 290.

Niazi, S., & Doroodgar, F. (2022). Fundamentals of Femtosecond Laser and Its Application in Ophthalmology. In S. W. Harun (Ed.), *Terahertz, Ultrafast Lasers and Their Medical and Industrial Applications.* IntechOpen. doi:10.5772/intechopen.106701

Nommeots-Nomm, A., Boetti, N., Salminen , T., Massera, J., Hokka, M., & Petit, L. (2018). Luminescence of Er^{3+} doped oxyfluoride phosphate glasses and glass-ceramics. *Journal of Alloys and Compounds, 751*, 224-230.

Ohja, N., Bogdan, M., Galatus, R., & Petit, L. (2020). Effect of heat-treatment on the upconversion of $NaYF_4$:Yb^{3+}, Er^{3+} nanocrystals containing silver phosphate glass. *Journal of Non-Crystalline Solids, 544, 120243*.

Ohja, N., Dmitrieva, I., Blanc, W., & Petit, L. (2021). Tailoring the Glass Composition to Increase the Thermal Stability without Impacting the Crystallization Behavior of Oxyfluorophosphate Glass. *Ceramics, 4*, 148-159.

Ohring, M. (1995). *Engineering Materials Science* (1st ed.). Hoboken, New Jersey: Elsevier Science & Technology.

Parang, Z., Keshavarz, A., Farahi, S., Elahi, S., Ghoranneviss, M., & Parhoodeh, S. (2012). Fluorescence emission spectra of silver and silver/cobalt nanoparticles. *Scientia Iranica, 19*(3), 934-947.

Patel, C. (1964). Continuous-Wave Laser Action on Vibrational-Rotational Transitions of CO_2. *Physical Review, 136*(5A), A1187-A1193.

Petit, L. (2019). Radiation effects on phosphate glasses: Review. *International journal of Applied Glass Science, 11*(3), 511-521.

Qi, J., Xu, T., Wu, Y., Shen, X., Dai, S., & Xu, Y. (2013). Ag nanoparticles enhanced near-IR emission from Er^{3+} ions doped glasses. *Optical MAterials, 35*, 2502-2506.

RP Photonics. (2007). *Dispersion Compensation*. Retrieved August 21, 2023, from https://www.rp-photonics.com/dispersion_compensation.html

RP Photonics. (2023). *Where to Buy Mode-locked Lasers*. Retrieved August 18, 2023, from https://www.rp-photonics.com/bg/buy_mode_locked_lasers.html

RP Photonics Encyclopedia. (2005). *CO_2 Lasers*. Retrieved 07 19, 2023, from https://www.rp-photonics.com/co2_lasers.html

RP Photonics Encyclopedia. (2005). *Femtosecond Lasers*. Retrieved August 11, 2023, from https://www.rp-photonics.com/femtosecond_lasers.html

RP Photonics Encyclopedia. (2006). *Passive mode locking*. Retrieved 08 13, 2023, from https://www.rp-photonics.com/passive_mode_locking.html

Schauer, K. (2021). *Laser Communications: Empowering More Data Than Ever Before*. Retrieved November 21, 2023, from https://www.nasa.gov/technology/laser-communications-empowering-more-data-than-ever-before/

Shelby, J. E. (2005). *Introduction to Glass Science and Technology* (2 ed.). Cambridge: Royal Society of Chemistry.

Shestopalova, I., Korri, J., Lemiere, A., Närhi, M., Gumenyuk, R., Boussard-Plédel, C., Troles, J., Petit, L. (2023). Addition of Ag_2O in Er^{3+} doped oxyfluorophosphate glass to allow the drawing of optical fibers. *Ceramics International - E-pub ahead of print*.

Stone, A., Sakakura, M., Shimotsuma, Y., Stone, G., Gupta, P., Miura, K., Hirao, K., Dierolf, V., Jain, H. (2009). Directionally controlled 3D ferroelectric single crystal growth in $LaBGeO_5$ glass by femtosecond laser irradiation. *Optics Express, 17*(25), 23284-23289.

Szczodra, A., Mardoukhi, A., Hokka, M., Boetti, N. G., & Petit, L. (2019). Fluorine losses in Er^{3+} oxyfluoride phosphate glasses and glass-ceramics. *Journal of Alloys and Compounds, 797*, 797-803.

University of Colorado. (2023). *Materials Instrumentation and Multimodal Imaging Core Facility*. Retrieved May 25, 2023, from https://www.colorado.edu/facility/mimic/instruments/renishaw-invia-raman-microscope

Veselský, K., Lahti, V., Petit, L., Prajzler, V., Šulc, J., & Jelínková, H. (2021). Influence of Y_2O_3 Content on Structural, Optical, Spectroscopic, and Laser Properties of Er^{3+}, Yb^{3+} Co-Doped Phosphate Glasses. *materials, 14*(14), 4041.

Yamane, M., & Asahara, Y. (2000). *Glasses for Photonics.* Cambridge: Cambridge University Press.

Zoubir, A. (2004). Towards Direct Writing Of 3-d Photonic Circuits Using Ultrafast Lasers. Orlando, Florida: University of Central Florida.